12-7-2012 12:00 AM

Nucleoredoxin and Wnt signaling in F9 cells

Leanne Sandieson
The University of Western Ontario

Supervisor
Dr. Greg Kelly
The University of Western Ontario

Graduate Program in Developmental Biology
A thesis submitted in partial fulfillment of the requirements for the degree in Master of Science

Nucleoredoxin and Wnt signaling in F9 cells

(Spine title: Nucleoredoxin and Wnt signaling in F9 cells)

(Thesis format: Monograph)

by

Leanne Sandieson

Graduate Program in Developmental Biology

A thesis submitted in partial fulfillment
of the requirements for the degree of
Master of Science

The School of Graduate and Postdoctoral Studies
The University of Western Ontario
London, Ontario, Canada

THE UNIVERSITY OF WESTERN ONTARIO
School of Graduate and Postdoctoral Studies

CERTIFICATE OF EXAMINATION

Supervisor

_____
Dr. Greg Kelly

Supervisory Committee

_____
Dr. Robert Cumming

_____
Dr. Jim Karagiannis

Examiners

_____
Dr. Robert Cumming

_____
Dr. Sashko Damjanovski

_____
Dr. Hugh Henry

The thesis by

Leanne Sandieson
entitled:

Nucleoredoxin and Wnt signaling in F9 cells

is accepted in partial fulfillment of the
requirements for the degree of
Master of Science

_____
Date

_____
Chair of the Thesis Examination Board

Abstract

Nucleoredoxin is a redox sensitive protein recently shown to be involved in the Wnt/β-catenin pathway through binding dishevelled. When Wnt is present, dishevelled prevents a destruction complex from degrading β-catenin. This facilitates the translocation of β-catenin into the nucleus where it binds to TCF-LEF to impart changes in gene expression. This study used mouse F9 cells as a model to examine whether or not nucleoredoxin is involved in augmenting the Wnt/β-catenin signaling required for extraembryonic endoderm differentiation. It was found that nucleoredoxin and three dishevelled isoforms were present in F9 cells. Furthermore, nucleoredoxin was found to bind to dishevelled-2, and when cells were treated with an oxidizing agent this interaction diminished. Lastly, when nucleoredoxin expression was knocked down, F9 cells differentiated into extraembryonic endoderm. Together, the data would indicate that the Wnt/β-catenin signaling pathway obligatory for extraembryonic endoderm differentiation is redox regulated at the level of nucleoredoxin.

Keywords

F9, Primitive endoderm, Parietal endoderm, Extraembryonic endoderm, ROS, H_2O_2, Differentiation, Dishevelled, Nucleoredoxin

Acknowledgements

First and foremost I would like to thank my supervisor Dr. Greg Kelly for his support and guidance. His endless encouragement and wisdom showed me how to become a confident and devoted researcher. He was supportive throughout my project and I am greatly appreciative for the experiences I have gained during my time in his lab.

I would like to thank the past and present members of the Kelly Lab in particular Greg Golenia, Steven Sun and Shaun Symons. I would like to extend a special thanks to Jason Hwang for his continuous support and guidance. His advice and valuable input on my research were essential throughout my project.

I also would like to thank my advisors Dr. Robert Cumming and Dr. Jim Karagiannis for their advice and technical assistance with this project. I would like to further thank Dr. Cumming for his extended guidance and for the use of his equipment. I would also like to thank Dr. Damjanovski for his support and use of his equipment.

Finally, I would like to thank current and previous members of the Cumming and Damjanovski labs including Mario Cepeda, Mark Fox, Michelle Nieuwesteeg, Tyler Cann and Jordan Epstein for their helpful advice, sharing of reagents and friendships throughout my project.

Table of Contents

List of Figures

List of Abbreviations

℃	Degrees Celsius
µg	microgram
µL	microliter
µm	micrometer
ANOVA	Analysis Of Variance
APC	Adenomatous Polyposis Coli
ATCC	American Type Culture Collection
β	beta
BSA	Bovine Serum Albumin
cDNA	complimentary Deoxyribonucleic Acid
CK1	Casein Kinase 1
CO_2	Carbon Dioxide
Ct	Cycle threshold
CXXC	Cysteine-X-X-Cysteine
db-cAMP	dibutyryl cyclic Adenosine Monophosphate
DMEM	Dulbecco's Modified Eagle's Medium
DMSO	Dimethyl Sulfoixde
DPI	Diphenyleneiodonium

DTT	Dithiothreitol
Dvl	Dishevelled
EMT	Epithelial-Mesenchymal Transition
ExE	Extraembryonic Endoderm
F9	Mouse F9 Embryonal Carcinoma (Teratocarinoma)
FBS	Fetal Bovine Serum
Fig	Figure
Fzd	Frizzled
GSK-3β	Glycogen Synthase Kinase 3 beta
h	hours
H_2O_2	Hydrogen Peroxide
HRP	Horseradish Peroxidase
HSD	Honestly Significant Difference
ICM	Inner Cell Mass
IgG	Immunoglobulin G
JNK	c-Jun-N-terminal Kinase
kDa	Kilodalton
LRP	Lipoprotein-receptor Related Protein
mins	minutes

M	Molar
mM	millimolar
MMTV	Mouse Mammary Tumor Virus
mRNA	messenger Ribonucleic Acid
NAC	N-Acetyl Cysteine
NIH3T3	Mouse embryonic fibroblast cell line
nM	nanomolar
NOX	NADPH Oxidase
NP-40	Nonyl Phenoxypolyethoxylethanol
NRX	Nucleoredoxin
PAGE	Polyacrylamide Gel Electrophoresis
PBS	Phosphate Buffered Saline
PCP	Planar Cell Polarity
PE	Parietal Endoderm
PrE	Primitive Endoderm
p-value	probability value
qRT-PCR	quantitative Reverse Transcription Polymerase Chain Reaction
RA	*all trans* Retinoic Acid
RNAi	Ribonucleic Acid interference

ROS	Reactive Oxygen Species
RT-PCR	Reverse Transcription Polymerase Chain Reaction
s	seconds
SDS	Sodium Dodecyl Sulphate
shRNA	small hairpin Ribonucleic Acid
SPSS	Statistical Package for the Social Sciences
TBS	Tris Buffered Saline
TBS-T	Tris Buffered Saline with Tween-20
TCF-LEF	T-Cell specific transcription Factor-Lymphoid Enhancer binding Factor
TM	Thrombomodulin
TROMA-1	Trophectoderm Monoclonal Antibody-1
TRX	Thioredoxin
VE	Visceral Endoderm
WNT	Wingless/ MMTV Integrated site

Chapter 1

1 Introduction

1.1 Early mouse development

During early mouse embryonic development, the fertilized egg undergoes a series of mitotic divisions leading to the development of the morula [1]. Cells of the morula give rise to one of two blastocyst lineages: trophectoderm or inner cell mass (ICM). The trophectoderm arises from the outer cells of the blastocyst and is responsible for the development of the embryonic placenta. The inner cells of the blastocyst form the ICM, which further differentiates into the epiblast, giving rise to the embryo proper, or to primitive endoderm (PrE) [1, 2] (Fig 1.1).

PrE further differentiates to parietal and visceral endoderms (PE and VE), which form the parietal and visceral yolk sacs, respectively. The cells of the PrE, PE and VE, collectively known as extraembryonic endoderm (ExE), are important for embryonic patterning as well as for providing nutrients and signaling molecules to the developing embryo [1, 3]. This differentiation of the ICM first to PrE and then to PE and VE is one of the earliest epithelial-to-mesenchymal transitions (EMT) in the developing mouse embryo. EMTs are characterized by the loss of E-cadherin expression, which eliminates stable junctions between the cells, and allows for the development of a morphological state suitable for cellular migration [4]. Analysing EMTs can provide insight into developmental processes as well as tumour progression and cancer metastasis.

Figure 1.1 Specified cells of the inner cell mass of the blastocyst differentiate first to primitive endoderm and then to parietal and visceral endoderm. In early mouse embryonic development, the blastocyst gives rise to cells of the inner cell mass (ICM). The ICM differentiates to either the epiblast, giving rise to the embryo proper, or to primitive endoderm (PrE). PrE further differentiates to parietal and visceral endoderms (PE and VE), which form the parietal and visceral yolk sacs, respectively (Image modified from [5]).

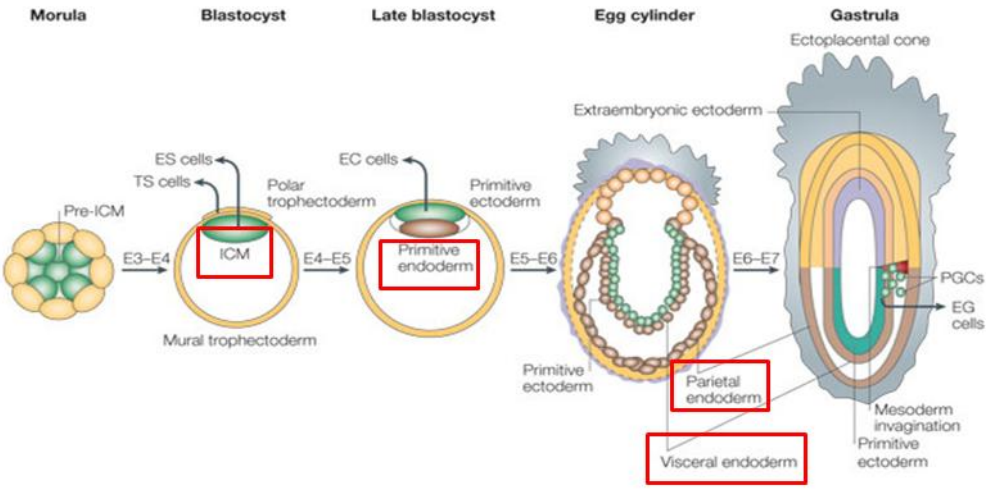
Morula
Blastocyst
Late blastocyst
Egg cylinder
Gastrula
Ectoplacental cone
Extraembryonic ectoderm
ES cells
TS cells
Polar trophectoderm
EC cells
Primitive ectoderm
Pre-ICM
E3–E4
ICM
E4–E5
Primitive endoderm
E5–E6
E6–E7
PGCs
EG cells
Mural trophectoderm
Primitive ectoderm
Parietal endoderm
Mesoderm invagination
Primitive ectoderm
Visceral endoderm

1.2 The mouse F9 teratocarinoma cell line

Studying EMTs, and in particular the transition to ExE, is difficult to study *in vivo.* Fortunately, researchers have been able to utilize the mouse F9 teratocarinoma cell line as a model to mimic this process *in vitro* [6, 7]. The F9 cell line was established by grafting 6-day old embryos into host testes of the mouse 129/Sv strain to produce teratomas [8]. Normally, these F9 teratocarcinoma cells undergo little differentiation, but when treated with retinoic acid (RA), a vitamin A derivative, the cells are induced to form PrE [9].

RA acts through binding to RA receptors and retinoid X receptors, which act as a heterodimer to efficiently bind RA-response elements in the promoter regions of target genes and transduce the retinoid signal [10, 11]. F9 cells have proven to be an important model for studying RA signaling as they express all known RA receptors. RA-responsive genes in F9 cells are numerous and include, but are not limited to, *Gata6, FoxA2* and *Wnt6* [11, 12]. When F9 cells are treated with low concentrations (10^{-7} M) of RA, changes in gene expression and cell morphology lead to the compact cells transitioning to a flat appearance as they move apart from one another, a scenario resembling PrE formation. Cytokeratin A intermediate filaments are also assembled and these can be detected using TROMA-1 **(**TROphectodermal Monoclonal Antibody) [13, 14]**.** RA signaling is therefore an essential regulator in cell differentiation and proliferation [4, 10].

F9 cells can be further induced to differentiate from PrE to PE by the addition of dibutyryl cyclic adenosine monophosphate (db-cAMP) to RA-treated cells. PE in the developing mouse embryo is in contact with the maternal blood; therefore PE should contain biological characteristics of vascular endothelial cells. Increasing the levels of

cAMP in F9 cells causes morphological changes as well as an increase in the secretion of tissue-type plasminogen activator and Thrombomodulin (TM), reminiscent of what occurs in the PE of mouse embryos [7, 14]. Accordingly, treating cells with RA followed by db-cAMP thus recapitulates the EMT of the ICM differentiating into ExE. In this study, TROMA-1 will be used as a pan-ExE marker while TM will be used as a marker exclusive to PE [13, 14].

1.3 Canonical Wnt/β-catenin signaling

Wnts are secreted glycoproteins that play numerous roles in vertebrate development including cell proliferation, cell survival, and determining cell fate [15]. In addition to development, Wnt pathways are also involved in cancers, neurodegenerative diseases, the regulation of bone density, and osteoarthritis [15]. There are nineteen known Wnts in vertebrates that signal through three pathways: canonical Wnt/β-catenin, planar cell polarity (PCP) or Wnt/Ca^{2+} pathway. My research focuses on canonical Wnt signaling as my lab reported several years ago that RA activates this specific pathway in F9 cells, and as a result cells differentiate to form ExE [16].

In the canonical Wnt/β-catenin pathway, Wnt binds to one of several seven-transmembrane Frizzled (Fzd) receptors, and to low-density lipoprotein-receptor related protein (LRP) 5/6. The binding of Wnt to its receptor causes Dishevelled (Dvl) to be recruited to the plasma membrane where it acts to inhibit a destruction complex composed of casein kinase 1 (CK1), glycogen synthase kinase 3 beta (GSK-3β), Axin, and the adenomatous polyposis coli tumour suppressor protein (APC). Disrupting this

complex allows β-catenin to accumulate in the cytosol, followed by its subsequent translocation into the nucleus where it binds to T-cell-factor lymphoid enhancer factor (TCF-LEF) to induce the transcription of Wnt target genes [16]. The regulated activation and repression of Wnt target genes, such as *Snail1*, *cyclinD1* and *c-Myc*, allows for cell proliferation and differentiation to PrE [17]. In the absence of Wnt, however, Dvl is not recruited to the plasma membrane, and therefore cannot disrupt the destruction complex. This results in cytoplasmic β-catenin being ubiquitinated by an E3 ubiquitin ligase and targeted for proteasomal destruction (Fig 1.2).

1.4 Reactive Oxygen Species

Recently, our lab has found that the RA-induced activation of canonical Wnt signaling in F9 cells and subsequent PrE formation is accompanied by increased reactive oxygen species (ROS) levels [18]. Not surprisingly, while increasing β-catenin levels is sufficient to induce PrE, it has been known for several years that other mechanisms are necessary to maintain cells in this state [6]. ROS is a term used to describe various species such as superoxides, hydrogen peroxide, and hydroxyl radicals. The most common production of ROS are as by-products from the incomplete reduction of oxygen through cellular respiration [19, 20]. More recent evidence shows ROS are also produced through NADPH oxidases (Nox), a plasma membrane-coupled enzyme complex that generates O_2^- using cytosolic NADPH as an electron donor [19].

Figure 1.2 Canonical Wnt/β-catenin signaling in F9 cells induces differentiation to PrE. Wnt binds to one of several Frizzled receptors, and to low-density lipoprotein-receptor related protein 5/6. This interaction causes Dishevelled (Dvl) to be phosphorylated and recruited to the plasma membrane where it acts to inhibit a destruction complex, thereby allowing β-catenin to accumulate in the cytosol and subsequently translocate to the nucleus where it binds to T-cell-factor lymphoid enhancer factor to induce the transcription of Wnt target genes necessary for PrE differentiation. In the absence of Wnt, Dvl is not recruited to the plasma membrane, and therefore it is unable to disrupt the destruction complex. As a result, β-catenin is targeted for proteasomal destruction.

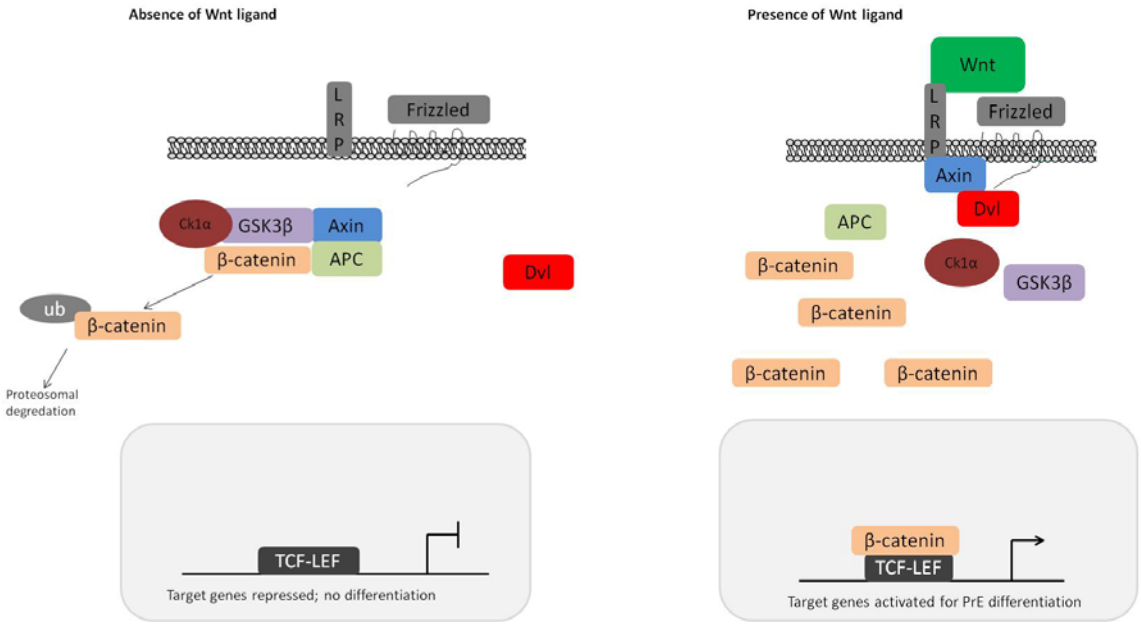
Absence of Wnt ligand
L
R
P
Frizzled
Ck1α
GSK3β
Axin
β-catenin
APC
Dvl
ub
β-catenin
Proteosomal
degredation
TCF-LEF
Target genes repressed; no differentiation
Presence of Wnt ligand
Wnt
L
R
P
Frizzled
Axin
Dvl
APC
β-catenin
Ck1α
GSK3β
β-catenin
β-catenin
β-catenin
β-catenin
TCF-LEF
Target genes activated for PrE differentiation

ROS are known to have deleterious effects causing damage to nucleic acids, proteins and lipids, however, antioxidants within the cell are able to regulate ROS levels to minimize this damage [21-23]. Besides deleterious effects, convincing studies indicate that cells use ROS in a beneficial manner to induce biological changes, including differentiation, proliferation, and apoptosis [24]. In particular, one ROS, hydrogen peroxide (H_2O_2) acts on the Wnt pathway to stimulate differentiation [25]. Our lab recently reported that F9 cells treated with H_2O_2 show morphological and molecular changes similar to that of RA treatment, causing cells to differentiate into PrE [18] [Hwang and Kelly, unpublished]. Together the data indicate that ROS are involved in crosstalk with the canonical Wnt/β-catenin pathway during ExE differentiation. The desire to better understand how this crosstalk augments Wnt signaling forms the basis of my thesis.

1.5 Nucleoredoxin and Dishevelled

Our lab has reported that when F9 cells are treated with RA to induce differentiation to PrE, there is an accompanied increase in ROS levels [18]. Furthermore, in the absence of RA, F9 cells treated with H_2O_2 differentiate to PrE. Interestingly, this work also highlighted the importance of ROS in the differentiation process as reducing ROS levels with antioxidants attenuates differentiation [18]. The mechanism by which ROS acts on PrE differentiation is unknown, but evidence from other systems and tissue culture models suggests that it may involve Nucleoredoxin (NRX).

Amino acid sequence similarity indicates that NRX is part of the Thioredoxin (TRX) family of redox proteins [26]. TRX is a ubiquitously expressed, evolutionarily conserved

protein containing a redox active site, Cysteine-X-X-Cysteine (CXXC). TRX catalyzes NADPH dependent reductions of disulfide bridges and functions as a disulfide oxidoreductase. Under oxidizing conditions, the thiol functional group on the two cysteine residues form a disulfide bridge capable of changing protein function or protein-protein interactions [27]. In terms of TRX, this disulfide bridge can be reduced by thioredoxin reductase and NADPH.

Evidence from whole-mount *in situ* hybridizations studies using mouse embryos suggests that NRX plays a role in patterning various tissues/regions during embryogenesis [26, 28]. Specifically, these *in situ* patterns show strong *NRX* expression in the limb buds and somites [26]. To date reports detailing the effects of knocking out the *NRX* gene in mouse embryos indicate embryos are smaller than their littermates and exhibited craniofacial defects with short frontal regions [29, 30], but nothing is known regarding a role of NRX in ExE development. Recently, investigators using NIH3T3 cells have reported on the involvement of NRX in canonical Wnt signaling [31]. In this investigation, immunoprecipitation followed by mass spectrometry revealed that NRX was a major binding partner of Dvl-1.

In mammals there are three Dvl isoforms: Dvl-1, Dvl-2, and Dvl-3. All isoforms are expressed during embryonic development and all show a similar, broad expression pattern, which would suggest that they act in a functionally redundant manner [32]. Studies in mice show that the individual knockouts of Dvl-1, Dvl-2 or Dvl-3 remain viable, but display defects including, but not limited to social, vertebral, and cardiac abnormalities. In double knockout studies, however, the absence of Dvl isoforms leads to more severe phenotypes including embryonic lethality [33], which would indicate that the

remaining isoform is not capable of assuming the role(s) left vacant due to the knockout. Incidentally, F9 cells express all three Dvl isoforms, with Dvl-2 constituting 95% of the Dvl pool [34]. Therefore, for the purpose of my research, all three Dvl isoforms were analysed, but emphasis was placed on Dvl-2.

The structure of Dvl is conserved amongst the three isoforms and includes three main protein binding domains allowing for Dvl to interact with over 60 proteins [35]. The DIX domain located at the N-terminus is involved in binding to Axin, a negative regulator of Wnt signaling. A central PDZ domain is involved in binding a large number of proteins including CK1 and NRX [31]. Lastly, the DEP domain, located at the C-terminus of Dvl, is thought to function in G-protein signaling [32].

1.6 Role of Nucleoredoxin in development and rationale for further research

At the onset of my study, the report of an increase in ROS levels following RA treatment of F9 cells, and the ability of H_2O_2 to induce differentiation in an RA-independent manner [18] left many unanswered questions. Interestingly, recent studies demonstrating that redox regulated proteins act on the canonical Wnt pathway [31] point to a general phenomenon where ROS play a regulatory role in signal transduction events. Furthermore, the observation that the amount of Dvl-1-bound to NRX increases under reduced conditions, and decreases when cells are subjected to oxidizing conditions [31], would suggest that the redox state of the cell is key in the regulation of these events. In this manner, the binding of NRX to Dvl would be expected to augment the negative regulation of β-catenin in the Wnt pathway via the destruction complex. In contrast, when

cells are exposed to oxidizing conditions, NRX would dissociate from Dvl, allowing it to await the Wnt signal and transduce it by destabilizing the β-catenin destruction complex [31] (Fig. 1.3). Thus, in this model, NRX serves as an inhibitor in the canonical Wnt signaling pathway. This model is supported by evidence from *NRX* knockout studies, where $NRX^{-/-}$ causes perinatal lethality due to dysregulation of Wnt/β-catenin signaling [29, 35]. What these knockout studies do not explain is the fact that defects are noted later in development and not at earlier stages, where Wnt signaling is known to be involved in ExE formation.

1.7 Objectives and Hypothesis

The objective of this research was to further address the role of NRX and Wnt signaling during vertebrate early development with a specific focus on EMTs and ExE differentiation. Observations from our lab have shown that in F9 cells, RA induction of PrE differentiation causes an upregulation of *Wnt6* and activation of the canonical Wnt/β-catenin pathway. Furthermore, these changes are accompanied by an increase in the levels of ROS. Based on these results, together with results from the literature indicating that NRX dissociates from Dvl-1 when NIH3T3 cells are treated with H_2O_2, **I hypothesize that during RA-induced activation of the canonical Wnt pathway in F9 cells, the accompanied increase in ROS leads to dissociation of NRX from Dvl, thereby augmenting the accumulation of β-catenin in the nucleus that is necessary for ExE differentiation**. To examine the role of NRX in Wnt signaling and ExE differentiaton, the mRNA and protein expression profiles of *NRX, Dvl-1, Dvl-2* and *Dvl-3*

in undifferentiated and RA treated F9 cells were determined. Next, co-immunoprecipitation assay was used to investigate the relationship between NRX and Dvl-2 under reducing and oxidizing condition. Finally, sh-*NRX* was used to knock down NRX to assess the effects on ExE formation.

Figure 1.3 Increase in ROS causes NRX dissociation from Dvl and enhances canonical Wnt signaling. Recent evidence suggests that in the absence of Wnt, NRX binds to Dvl and augments the negative regulation of β-catenin via the destruction complex. Following an increase in ROS, the thiol functional group on the two cysteine residues of NRX form a disulfide bridge, changing the conformation of NRX, thereby allowing it to dissociate from Dvl. This release of Dvl inactivates the destruction complex, thus allowing β-catenin to accumulate and subsequently translocate to the nucleus where it binds to TCF-LEF to induce Wnt target genes.

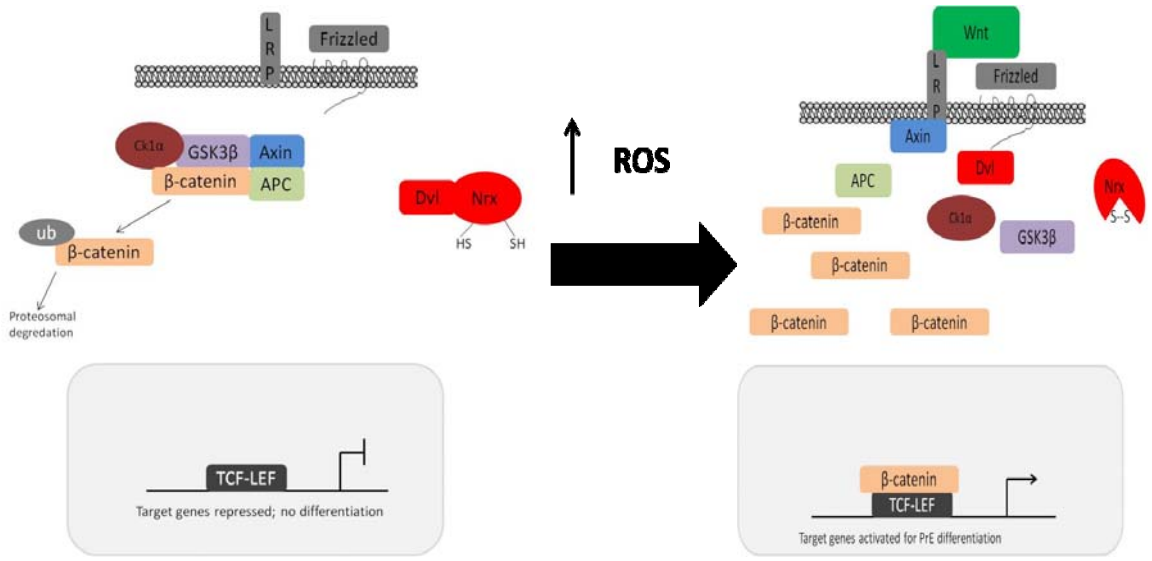
L
R
P
Frizzled
Ck1α
GSK3β
Axin
β-catenin
APC
ub
β-catenin
Proteosomal
degredation
Dvl
Nrx
HS
SH
ROS
Wnt
L
R
P
Frizzled
Axin
Dvl
APC
Nrx
S–S
β-catenin
Ck1α
GSK3β
β-catenin
β-catenin
β-catenin
TCF-LEF
Target genes repressed; no differentiation
β-catenin
TCF-LEF
Target genes activated for PrE differentiation

Chapter 2

2 Materials and Methods

2.1 Cell Culture

F9 cells (ATCC) were cultured in Dulbecco's modified Eagle's medium (Gibco) supplemented with 1 % penicillin-streptomycin (Gibco) and 10 % fetal bovine serum (Gibco) and incubated at 37^{o}C and 5 % CO_2. Cells were treated with dimethyl sulphoxide (DMSO), serving as a control, 10^{-7} M retinoic acid (RA all-trans; Sigma), or 0.05 mM and 0.1 mM H_2O_2 (EMD). Further analysis of cell differentiation was tested using RA plus 0.05 mM dibutyryl cyclic adenosine monophosphate (db-cAMP; Sigma), or H_2O_2 and db-cAMP.

For antioxidant analysis, F9 cells were first treated with 1 mM and 2 mM *N*-Acetyl-L-cysteine (NAC; Sigma), or 0.1 mM and 0.5 mM L-Ascorbic acid (Vitamin C; Sigma) for 24 h, and then treated with 10^{-7} M RA. NAC, Vitamin C and RA were replenished every day for 3 days.

2.2 Reverse Transcription PCR and Quantitative Reverse Transcription PCR

Total RNA was collected using the RNeasy kit (Qiagen) and converted into first strand cDNA using reverse transcriptase qScript cDNA Supermix (Quanta). RNA was isolated following treatment of F9 cells with DMSO, RA (for 1, 2, 3 and 4 days), H_2O_2 (for 1, 2, and 3 days) or RA/H_2O_2 and db-cAMP. Primers were designed to: *L14* sense

(5’GGGAGAGGTGGCCTCGGACGC) and antisense (5’GGCTGGCTTCACTCAAAGGCC) to produce a 300 bp product. *L14* is a constitutively expressed gene in F9 cells and used as an internal control. *NRX* sense (5’ TCTGCTCACCATTCTGGACA) and antisense (5’ACACGCTGGAAAAGTCCAAG) to produce a 200 bp product, *Gata6* sense (5’CTCTGCACGCTTTCCCTACT) and antisense (5’GTAGGTCGGGTGATGGTGAT) to produce a 200 bp product, *FoxA2* sense (5’ACCTGAGTCCGAGTCTGAGC) and antisense (5’CATGGTGATGAGCGAGATGT) to produce a 200 bp product, *TM* sense (5’CCAGGCTCTTACTCCTGTA) and antisense (5’TGGCACTGAAACTCGCAGTT) to produce a 200 bp product. Primers were also designed for *Dvl-1* sense (5’CATCCTCCTTCAGCAGCATCAC) and antisense (5’ACTCGTACCATAGCGGGGC) to produce a 450 bp product, *Dvl-2* sense (5’AGACTCGGATGAGGATGACA) and antisense (5’AAGGCTCCAGTCAGCGCA) to produce a 550 bp product, and *Dvl-3* sense (5’TGGGGCTGTGGCAGCTGATGG) and antisense (5’GAGGCCATGGCTTTTACGATG) to produce a 400 bp product [36].

Primers were used with first strand cDNA template for reverse transcriptase-polymerase chain reaction (RT-PCR) using a thermocycler (Eppendorf) and the following conditions: *NRX* – 35 cycles of 30 s at 94^{o}C, 30 s at 55^{o}C, and 30 s at 72^{o}C; *Dvl-1* – 40 cycles of 30 s at 94^{o}C, 30 s at 55^{o}C, and 30 s at 72^{o}C; *Dvl-2* – 38 cycles of 30 s at 94^{o}C, 30 s at 55^{o}C, and 30 s at 72^{o}C; *Dvl-3* – 42 cycles of 30 s at 94^{o}C, 30 s at 60^{o}C, and 30 s at 72^{o}C; *Gata6* – 35 cycles of 30 s at 94^{o}C, 30 s at 57^{o}C, and 30 s at 72^{o}C; *FoxA2* – 35 cycles of 30 s at 94°C, 30 s at 58°C, and 30 s at 72°C; *TM* – 32 cycles of 30 s at 94^{o}C, 30 s at 57^{o}C, and 30 s at 72^{o}C . PCR products were analyzed on 1 % agarose gels containing

ethidium bromide and DNA was visualized using a FluorChem 8900 Gel Doc System (Alpha Innotech). All amplicons were sequenced at the Roberts' Research Institute (UWO), to confirm their identity.

Quantitative reverse transcription-PCR (qRT-PCR) analysis was carried out in triplicate using the Rotor Gene 3000 (Corbett). Each reaction contained 1 μL of cDNA, 500 nM concentrations of each of the primers described above, and a PerfeCTa SYBR green PCR Fastmix (Quanta Biosciences). Gene expression analysis was performed using the comparative cycle threshold (Ct) method, normalized to *L14* expression, and the fold changes were calculated relative to control DMSO-treated cells.

2.3 Immunoblot Analysis

Protein lysates were collected in 2 % sodium dodecyl sulfate (SDS) buffer containing 0.5 M Tris-HCl pH 6.8 (BioShop), 5 % glycerol, 5 % 2-mercaptoethanol (BDH), 2 % SDS (BioShop) and 1 % Halt Protease Inhibitor Cocktail (Thermo Scientific). Protein concentrations were determined using a Bradford Assay (Bio-Rad). Approximately 40 μg of protein were separated on denaturing 10 % polyacrylamide gels for 1.5 h at 120 volts. Following electrophoresis, the proteins were electrophoretically transferred for 1 h to nitrocellulose membranes (Biotrace; Pall Corp.) using Tris-glycine transfer buffer containing 20 % methanol. The membranes were blocked in Tris buffered saline containing 0.1 % Tween 20 (TBS-T) and 5 % skim milk for 1 h at room temperature. Membranes were then probed with primary antibody(s) overnight at 4^{o}C followed by 3 washes in TBS-T, and then probed with secondary antibody(s) for 2 h at

room temperature. Signals were detected using the SuperSignal West Pico Chemiluminescent Detection Kit (Pierce) and X-Omat Blue XB-1 Film (Kodak) or captured on a Molecular Imager Gel Doc XR System (BioRAD) and imaged using Quantity One Software. The primary antibodies were directed against TROMA-1 (1:10; 55 kDa, Developmental Studies Hybridoma Bank), β-Actin (1:10000; 47 kDa, Santa Cruz), NRX (1:250; 55 kDa, Santa Cruz), Dvl-1 (1:250; 85 kDa, Santa Cruz), Dvl-2 (1:250; 92 kDa, Santa Cruz) and Dvl-3 (1:200; 81 kDa, Santa Cruz) and dissolved in 5 % Bovine Serum Albumin (BSA; OmniPur) and TBS-T. Secondary antibodies including HRP-conjugated anti-goat, anti-rat and anti-mouse (1:5000; Pierce) were dissolved in 5 % skim milk and TBS-T.

2.4 Co-Immunoprecipitation

Cells grown to approximately 80 % confluency were treated with 1 mM dithithreitol (DTT; New England BioLabs) or 1 mM H_2O_2 for 15 min and protein lysates were collected in nonyl phenoxypolyethoxylethanol-40 lysis buffer (NP-40) containing 50 mM Tris pH 7.2 (BioShop), 100 mM NaCl (BioShop), 0.1 % IGEPAL (Sigma), 10 % glycerol, 1 mM ethylenediaminetetraacetic acid (EDTA; Gibco) and 0.1 mM phenylmethylsulfonyl fluoride (PMSF; Sigma). Lysates were incubated in NP-40 lysis buffer for 10 minutes then passed through a 25-gauge needle 15 times and centrifuged for 10 min at 4ºC. To immunoprecipitate proteins bound to Dvl-2, protein lysate (2 mg/mL) was first pre-cleared using a 20 µL sepharose bead volume (Protein A/G PLUS Agarose Immunoprecipitation Reagent; Santa Cruz) for 1 h. Lysates were then treated overnight at

4ºC with either 1 µg of anti-Dvl-2 antibody or 1 µg of IgG normal mouse serum (Santa Cruz), as a control. Antibody-protein complexes were then immobilized on sepharose beads for 2 h at 4ºC. Bound proteins were washed three times with NP-40 lysis buffer, eluted from the beads using electrophoresis sample buffer (New England BioLabs), resolved by sodium dodecyl sulfate polyacrylamide gel electrophoresis (SDS-PAGE), and then blotted to nitrocellulose membrane. The membrane was blocked with TBS-T and 5 % skim milk for 1 h, and then probed with anti-NRX antibody (1:250) overnight at 4ºC and then with an HRP-conjugated anti-goat antibody (1:5000) for 2 h. To confirm the pull-down of Dvl-2, membranes were stripped and reprobed with anti-Dvl-2 antibody (1:250) and HRP-conjugated anti-mouse antibody (1:5000).

2.5 sh-*NRX* construct and Knockdown

The following sequence derived from the mouse *NRX* cDNA was used for the knockdown of *NRX*: (AA)GATCATTGCCAAGTACAAA [31]. Oligonucleotide primers designed to amplify the above sequence was used with PCR to clone the *NRX* sh-RNA into the pRS shRNA vector (a generous gift from Dr. Robert Cumming; sh-*NRX*). Cells were transfected with sh-*NRX*, or with pRS or CMV-GFP constructs as negative and transfection efficiency controls, respectively, using Lipofectamine 2000 and according to the manufacturer's protocol (Invitrogen). Briefly, F9 cells grown to approximately 90 % confluency were transfected with 10 uL of Lipofectamine 2000 and 4 ug of each of the constructs in 2 mL of Opti-MEM (Invitrogen). Opti-MEM was replaced with complete media 5 h post transfection and cells were cultured for 3 days. For differentiation to PE

analysis, Opti-MEM was replaced with complete media plus db-cAMP (0.05 mM). mRNA was collected using methods described previously (section 2.2), while protein lysates were collected in 2 % SDS lysis buffer.

2.6 Microscopy

Cells were examined under bright field using a Zeiss Axio Observer A1 inverted microscope and images were captured using a QImaging Retiga CCD camera. All images were assembled as plates using Adobe Photoshop CS3 and Adobe Illustrator CS3.

2.7 Statistical Analysis

Densitometric analyses of immunoblots and quantitative reverse transcription PCR data were compiled from three independent biological replicate experiments performed on separate occasions. Comparisons of data between the control and treated, or transfected groups were performed using a one-way ANOVA and Tukey's HSD post-hoc tests (SPSS). Data is presented as mean and standard error of the mean. The p values were one-sided and considered statistically significant at the 0.05 level.

Chapter 3

3 Results

3.1 RA, H_2O_2 and db-cAMP induce differentiation of F9 cells

Previous work in our lab has demonstrated an accompanied increase in ROS levels when F9 cells are treated with RA to induce PrE differentiation. Moreover, cells also differentiate to PrE when they are treated with H_2O_2 [18]. To confirm these results, cells were treated with RA or H_2O_2, and then examined for markers of differentiation. RA treatments were examined over a 4 day period and compared to DMSO-vehicle treated cells. Morphological analysis showed DMSO treatments caused cells to appear compact, while treatment with RA showed cells acquiring a more flattened morphology as they moved apart from one another. Similarities in morphology to RA-treated cells occurred when cells were treated with 0.1 mM H_2O_2 for 3 consecutive days (Fig. 3.1A).

Previous work has shown that the addition of db-cAMP to RA-treated F9 cells cause them to further differentiate to PE [7]. Although this ability to chemically induce F9 cells to form PE is well known, no report had documented whether H_2O_2 in the presence of db-cAMP would have the same outcome. To this end, F9 cells were treated with either RA or H_2O_2, and subsequently with db-cAMP. Results show that the addition of H_2O_2 and db-cAMP caused F9 cells to adopt a similar morphology as RA and db-cAMP. In each case cells that have moved away from the compact mass displayed extended protrusions and appeared more refractile than those exposed to RA or H_2O_2 alone (Fig. 3.1A).

Figure 3.1 RA and H_2O_2 induce morphological changes and markers of primitive endoderm; with the addition of db-cAMP cells become competent to form parietal endoderm. F9 cells were treated with DMSO, RA (10^{-7} M), H_2O_2 (0.1 mM), RA and db-cAMP (0.05 mM) or H_2O_2 and db-cAMP. (A) F9 cells treated with DMSO grow in tightly compact groups (top), whereas those treated with H_2O_2 show a flattened, more elongated morphology, similar to that of RA-treated cells (middle). H_2O_2-treated cells exposed to db-cAMP become refractile, and show extended protrusions reminiscent of RA and db-cAMP (bottom). (B) Immunoblot analysis for TROMA-1 shows expression induced by RA treatments, with the highest levels present on day 4. (C) Immunoblot analysis shows expression of TROMA-1 increased by H_2O_2 treatment, with the highest levels present on day 3. (D) RT-PCR analysis shows increased *TM* in cells treated with RA and db-cAMP and in those treated with H_2O_2 and db-cAMP. Data represents 3 independent experiments. Scale bars = 20 μm.

A

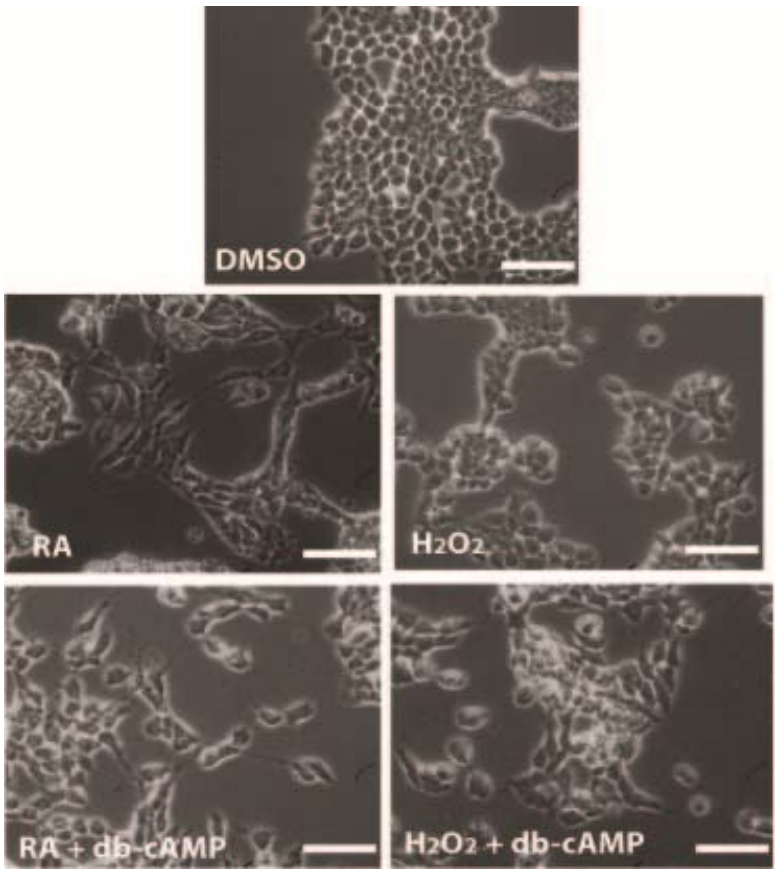
DMSO
RA
H2O2
RA + db-cAMP
H2O2 + db-cAMP

B

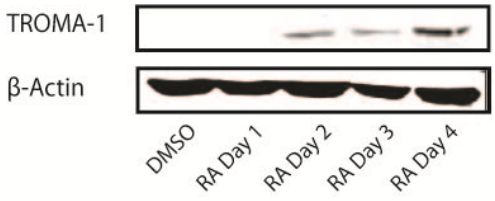
TROMA-1
β-Actin
DMSO
RA Day 1
RA Day 2
RA Day 3
RA Day 4

C

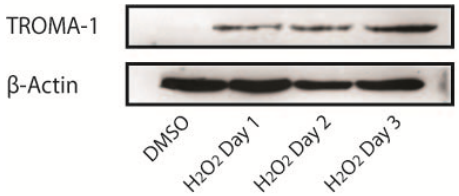
TROMA-1
β-Actin
DMSO
H2O2 Day 1
H2O2 Day 2
H2O2 Day 3

D

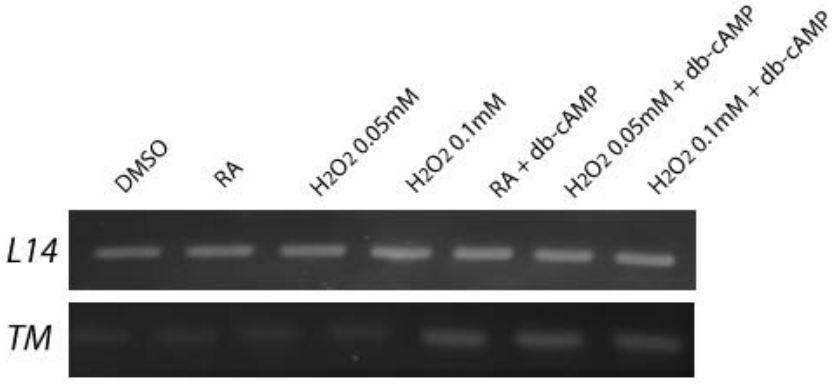
DMSO
RA
H2O2 0.05mM
H2O2 0.1mM
RA + db-cAMP
H2O2 0.05mM + db-cAMP
H2O2 0.1mM + db-cAMP
L14
TM

Immunoblot analysis, using the TROMA-1 antibody to detect the characteristic assembly of cytokeratin A intermediate filaments that is seen in PrE, was used to confirm the morphological changes that resulted from RA and H_2O_2 treatments. As expected, TROMA-1 signals were not seen in DMSO treated control cells, but were present after RA treatment, with the highest level after 4 days (Fig 3.1B). Likewise, a similar pattern of TROMA-1 staining was seen in H_2O_2 treated cells. DMSO had no effect on TROMA-1 levels, while treatment with H_2O_2 for 3 days caused an increase (Fig. 3.1C). These morphological and molecular results confirmed that F9 cells treated with either RA or H_2O_2 had differentiated into PrE [18].

Since H_2O_2 was able to take the place of RA and direct cells into the PrE lineage, the next question was to test whether these H_2O_2-induced cells were competent to further differentiate into PE. RT-PCR was used to detect *Thrombomodulin* (*TM*), a marker of PE differentiation. As expected, *TM* was not detected in DMSO, RA, or H_2O_2 treatments, but with the addition of db-cAMP the expression of *TM* increased (Fig. 3.1D). Together, these results indicated that H_2O_2/db-cAMP treatment was sufficient to induce F9 cells to form PE.

3.2 Antioxidants attenuate RA-induced differentiation

Studies from the Kelly lab have shown that increasing ROS levels in F9 cells is sufficient to induce them to differentiate into PrE, while blocking ROS production through addition of antioxidants inhibits differentiation [18]. To confirm these studies, F9 cells were treated with DMSO, RA or increasing concentrations (1 mM and 2 mM) of N-

Acetyl Cysteine (NAC) supplemented with RA. To determine if the block to differentiation was NAC-specific, F9 cells were also treated with various concentrations (0.1 mM and 0.5 mM) of the antioxidant ascorbic acid, the reduced form of Vitamin C, and then exposed to RA.

Immunoblot analysis showed no TROMA-1 signal when cells were treated with DMSO alone, but signals were seen in RA-treated cells (Fig. 3.2A). Compared to RA alone, cells treated with NAC or Vitamin C showed weaker TROMA-1 signals (Fig. 3.2A). Densitometry analysis comparing TROMA-1 levels relative to the β-actin loading control was performed. Results indicate that in comparison to RA, TROMA-1 levels decreased significantly in cells treated with 1 mM and 2 mM NAC and in those treated with 0.5 mM Vitamin C (Fig. 3.2B). While a concentration of 0.1 mM Vitamin C showed a decrease in TROMA-1, these levels were not found to be significant. As expected, cells treated with DMSO had TROMA-1 levels that were significantly lower than the RA, positive control. Together, these results indicate that exposure to antioxidants inhibits RA-induced differentiation of F9 cells into PrE, suggesting that ROS are necessary and sufficient for this to process to occur.

3.3 *Dvl-1, Dvl-2* and *Dvl-3* mRNA expression profiles remain constant after RA treatment

In the presence of Wnt, Dvl is recruited to the plasma membrane and acts to disassemble a destruction complex that otherwise would target β-catenin for proteasomal degradation. Since RA is known to affect the expression of many genes [11], including in

Figure 3.2 Antioxidants NAC and Vitamin C attenuate RA-induced differentiation in F9 cells. F9 cells were treated with NAC (1 mM and 2 mM) or Vitamin C (0.1 mM and 0.5 mM) for one day, and then treated with RA (10^{-7} M). Cells treated with DMSO or RA (10^{-7} M) served as a control. (A) Immunoblot analysis for TROMA-1 showing levels of endo-A cytokeratin in cells treated with RA, but not in the DMSO control. These levels decreased when cells were treated with NAC and then exposed to RA, or when treated with Vitamin C and then RA. (B) Densitometry analysis show that there was a significant decrease in the TROMA-1-positive signals in cells treated with NAC (1 mM and 2 mM) or Vitamin C (0.5 mM) and RA, compared to those treated with RA alone. TROMA-1 was not significantly different in cells treated with Vitamin C (0.1 mM) plus RA, compared to those treated with RA alone. Densitometry was calculated by comparing the TROMA-1/β-actin ratio of each treatment to the same ratio in the RA control treatment. Asterisks denote significant difference ($p \leq 0.05$). Data represents the mean and standard error of three independent experiments.

A

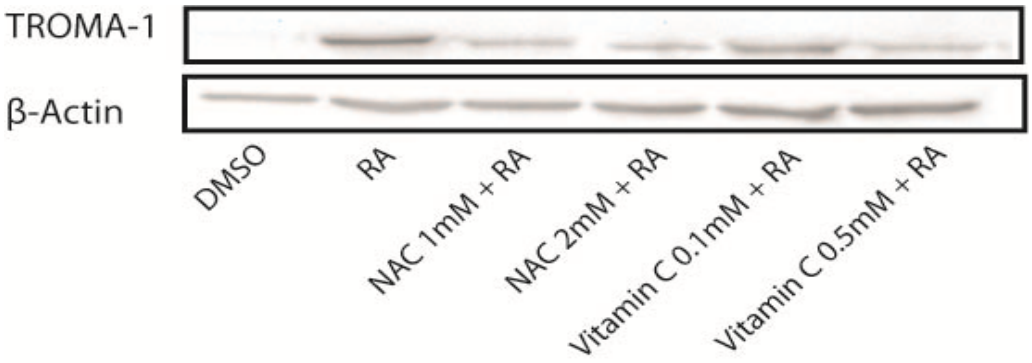
TROMA-1
β-Actin
DMSO
RA
NAC 1mM + RA
NAC 2mM + RA
Vitamin C 0.1mM + RA
Vitamin C 0.5mM + RA

B

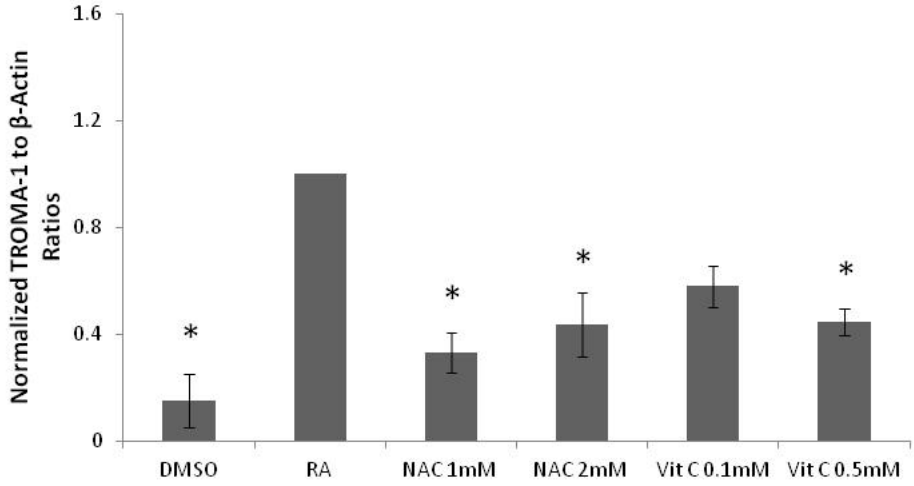
Normalized TROMA-1 to β-Actin Ratios
1.6
1.2
0.8
0.4
0
*
*
*
*
DMSO
RA
NAC 1mM
NAC 2mM
Vit C 0.1mM
Vit C 0.5mM

Wnt6 [16], the possibility exists that other members of the canonical Wnt signaling pathway, and in particular Dvl, may be regulated at either the mRNA or protein level in F9 cells treated with RA. To address this, the relative mRNA levels of all three Dvl isoforms were analysed to determine if the Dvl genes are RA-responsive.

The mRNA expression profile of *Dvl-1, Dvl-2* and *Dvl-3* was determined in cells treated with DMSO or RA for 1 to 4 days. RT-PCR was employed and amplicons confirmed that all three Dvl isoforms are present in F9 cells; however, relative levels appeared similar between the RA-treated and DMSO control cells (Fig. 3.3A-C). Since these levels appeared constant, it was necessary to use qRT-PCR to determine if subtle differences in expression exist. The expression levels of *Dvl-1, 2* and *3,* normalized to *L14*, was determined in RA-treated cells and compared to the vehicle control. Results confirmed there was no significant change in the expression levels of *Dvl-1, 2* or *3* in RA-treated cells compared to DMSO (Fig. 3.3D-F). To confirm these results, these mRNA expression levels were compared to that of a known RA-responsive gene, *Gata6* [12]. qRT-PCR results showed that *Gata6* expression increased at 1 day post-RA treatment and continued to increase significantly through day 4 (Fig. 3.3G). In light of the *Gata6* expression, it would appear that *Dvl-1, Dvl-2* and *Dvl-3* are not RA-responsive genes.

3.4 Dvl-1, Dvl-2 and Dvl-3 protein expression profiles remain constant after RA treatment

Since there were no obvious changes in the levels of *Dvl-1, 2* or *3* mRNA in response to RA, I decided to use immunoblot analysis to investigate Dvl-1, 2 and 3 protein levels

Figure 3.3 Dvl-1, Dvl-2 and Dvl-3 mRNA levels are not affected by RA treatment. F9 cells were treated with DMSO or RA (10^{-7} M) for 1 to 4 days and total RNA was collected, reverse transcribed into first strand cDNA, and used as template for PCR analysis with primers designed to *Dvl-1, Dvl-2* and *Dvl-3*. (A-C) Three separate RT-PCR experiments show all three *Dvl* genes are expressed in both DMSO and RA-treated cells. (D-F) qRT-PCR analysis shows that there was no significant difference in the transcript level of any *Dvl*. (G) qRT-PCR, with primers designed to *Gata6*, an RA-responsive gene, show that there is a significant increase in *Gata6* expression in cells following treatment with RA. For qRT-PCR analysis, the expression levels of *Dvl-1, -2, -3* and *Gata6* were normalized to *L14* and compared to the vehicle control. Asterisks denote significant difference ($p \leq 0.05$). Data represents the mean and standard error of three independent experiments.

A

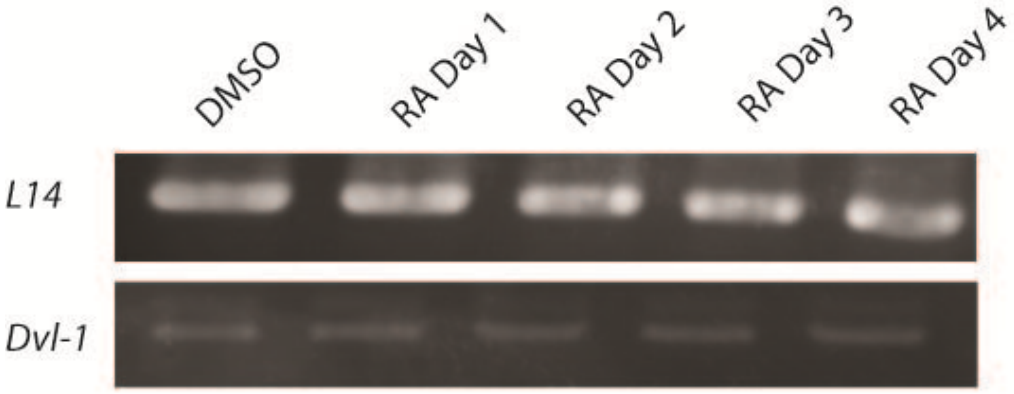
DMSO
RA Day 1
RA Day 2
RA Day 3
RA Day 4
L14
Dvl-1

B

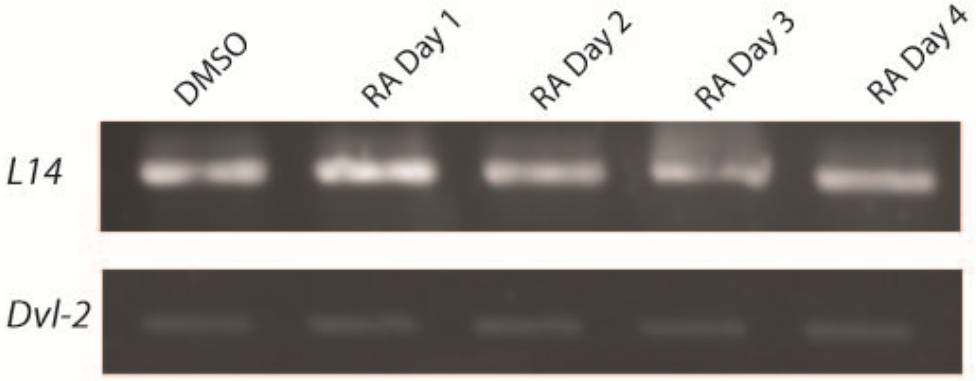
DMSO
RA Day 1
RA Day 2
RA Day 3
RA Day 4
L14
Dvl-2

C

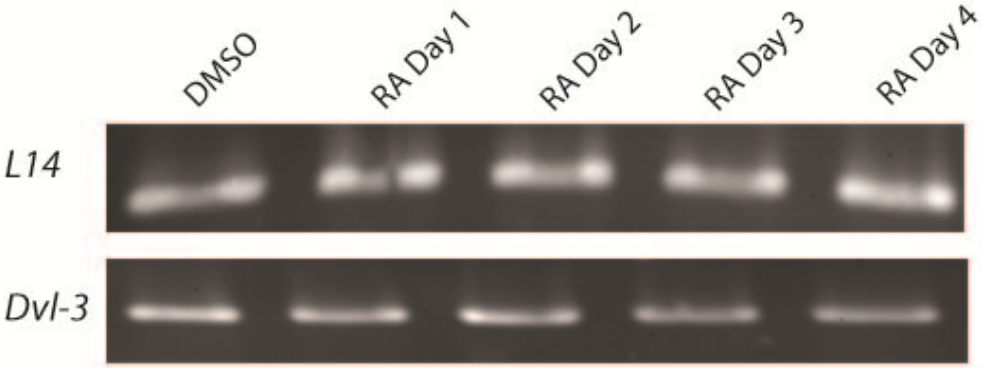
DMSO
RA Day 1
RA Day 2
RA Day 3
RA Day 4
L14
Dvl-3

D

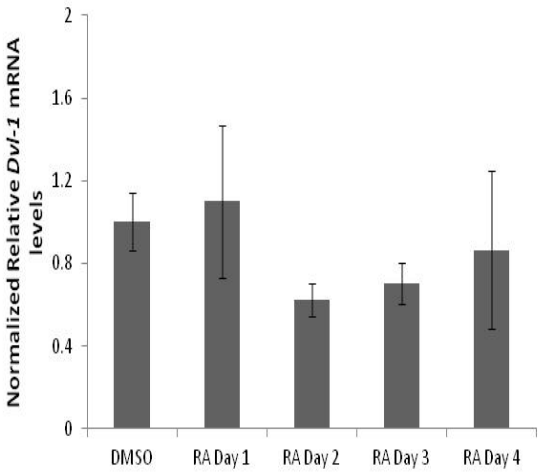
Normalized Relative Dvl-1 mRNA levels
2
1.6
1.2
0.8
0.4
0
DMSO
RA Day 1
RA Day 2
RA Day 3
RA Day 4

E

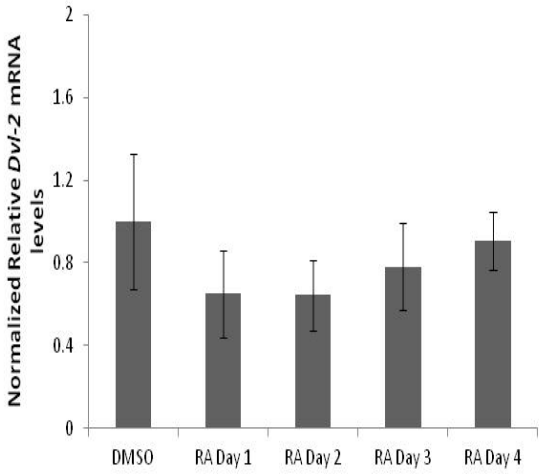
Normalized Relative Dvl-2 mRNA levels
2
1.6
1.2
0.8
0.4
0
DMSO
RA Day 1
RA Day 2
RA Day 3
RA Day 4

F

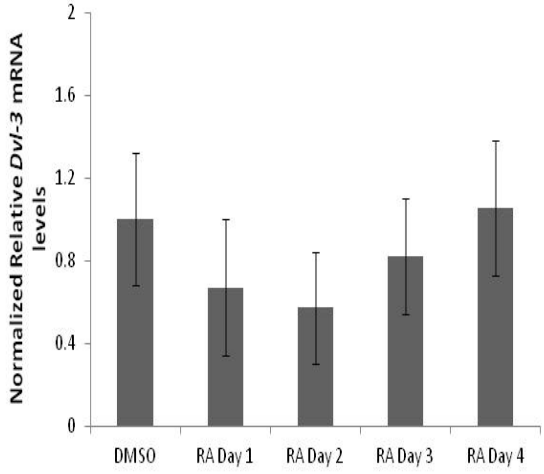
Normalized Relative Dvl-3 mRNA levels
2
1.6
1.2
0.8
0.4
0
DMSO
RA Day 1
RA Day 2
RA Day 3
RA Day 4

G

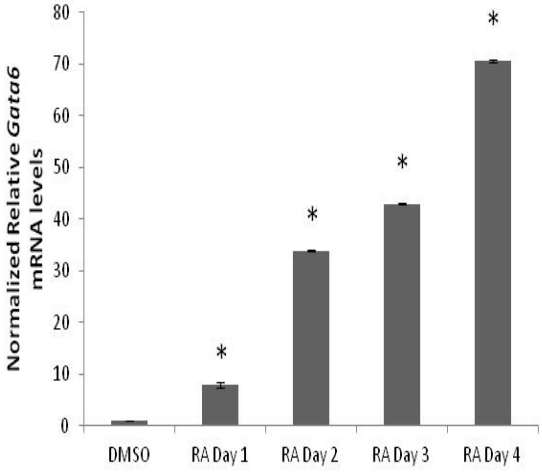
Normalized Relative Gata6 mRNA levels
80
70
60
50
40
30
20
10
0
*
*
*
*
DMSO
RA Day 1
RA Day 2
RA Day 3
RA Day 4

under the same conditions. Antibodies against each specific Dvl were used on blots containing proteins isolated from DMSO or RA-treated cells. A β-actin antibody was used to ensure equal loading between samples. Results show that Dvl-1, 2 and 3 were present in both vehicle-treated and RA-treated cells (Fig. 3.4A-C). Furthermore, densitometry analysis confirmed that there were no significant changes in the levels of each Dvl isoform in either DMSO or RA-treated cells (Fig. 3.4D-F).

3.5 *NRX* mRNA expression profile remains constant after RA treatment

Since Dvl was not RA-responsive as RA had no effect on the steady state levels of any of the three Dvl isoforms, the focus turned to NRX, a protein known to interact with Dvl [31] and one that is redox sensitive [26]. These results were particularly intriguing given the effects of treating F9 cells with H_2O_2 (described above in section 3.1). First, to determine if the expression of *NRX* changed in response to RA, cells were treated with RA for 1 to 4 days and total RNA was collected. The RNA was then reverse transcribed into first strand cDNA and used as a template for PCR with *NRX* specific primers. Results show that *NRX* was present in DMSO-treated (undifferentiated) F9 cells (Fig. 3.5A). Furthermore, the levels of *NRX* appeared to remain constant following RA treatment. qRT-PCR was used to determine if there were any subtle changes in *NRX* expression. Results, normalized to the vehicle control and compared to RA treatments at days 1 to 4, show that there were no significant changes in *NRX* expression between DMSO and RA-treated cells (Fig. 3.5B).

Figure 3.4 Dvl-1, Dvl-2 and Dvl-3 protein levels are not affected by RA treatment. F9 cells were treated with DMSO or RA (10^{-7} M) for 1 to 4 days and protein lysates were collected and used for immunoblot analysis with antibodies against Dvl-1, Dvl-2 and Dvl-3. (A-C) Immunoblot showing Dvl-1, Dvl-2, and Dvl-3 in DMSO and RA-treated F9 cells. Note that the relative levels of Dvl-1, Dvl-2 and Dvl-3 did not change following treatment. (D-F) Densitometry analysis confirms that there were no significant changes in Dvl-1, Dvl-2 or Dvl-3 protein levels following either DMSO or RA treatment. Densitometry was calculated by comparing the Dvl-1, -2, -3/β-actin ratio of each treatment to the same ratio in the vehicle control treatment. Asterisks denote significant difference ($p \leq 0.05$). Data represents the mean and standard error of three independent experiments.

A

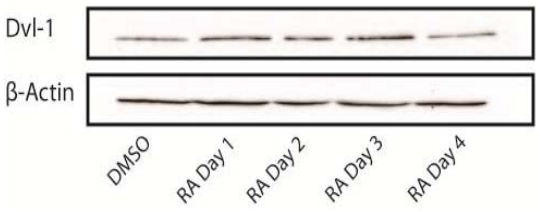
Dvl-1
β-Actin
DMSO
RA Day 1
RA Day 2
RA Day 3
RA Day 4

D

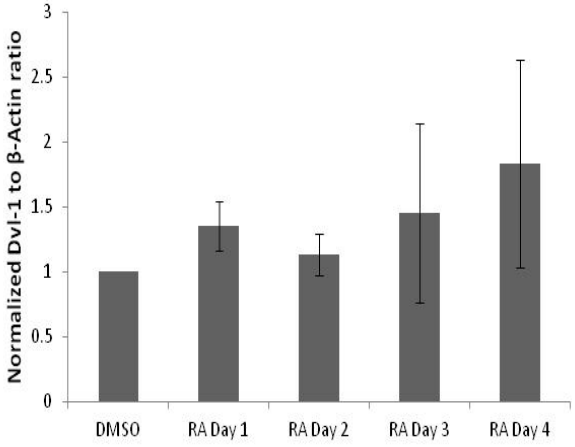
Normalized Dvl-1 to β-Actin ratio
3
2.5
2
1.5
1
0.5
0
DMSO
RA Day 1
RA Day 2
RA Day 3
RA Day 4

B

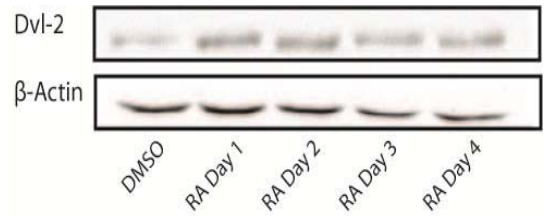
Dvl-2
β-Actin
DMSO
RA Day 1
RA Day 2
RA Day 3
RA Day 4

E

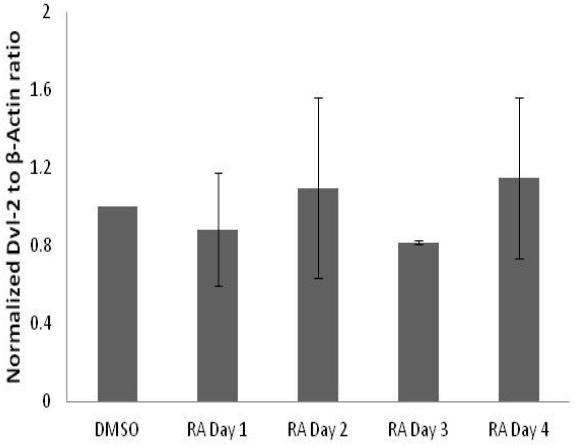
Normalized Dvl-2 to β-Actin ratio
2
1.6
1.2
0.8
0.4
0
DMSO
RA Day 1
RA Day 2
RA Day 3
RA Day 4

C


Dvl-3
β-Actin
DMSO
RA Day 1
RA Day 2
RA Day 3
RA Day 4

F

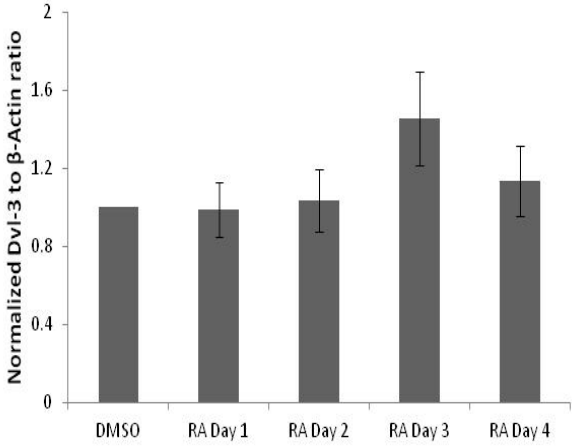
Normalized Dvl-3 to β-Actin ratio
2
1.6
1.2
0.8
0.4
0
DMSO
RA Day 1
RA Day 2
RA Day 3
RA Day 4

Figure 3.5 NRX mRNA levels are not affected by RA treatment. F9 cells were treated with DMSO or RA (10^{-7} M) for 1 to 4 days. Total RNA was collected, reverse transcribed into first strand cDNA, and used as template for PCR analysis with primers designed to *NRX*. (A) RT-PCR results show that the *NRX* mRNA transcript is present after treatment with DMSO or RA. (B) qRT-PCR data confirmed that there were no significant differences in mRNA transcript levels of *NRX* between treatments. For qRT-PCR analysis, the expression level of *NRX* was normalized to *L14* and compared to the vehicle control. Asterisks denote significant difference ($p \leq 0.05$). Data represents the mean and standard error of three independent experiments.

A

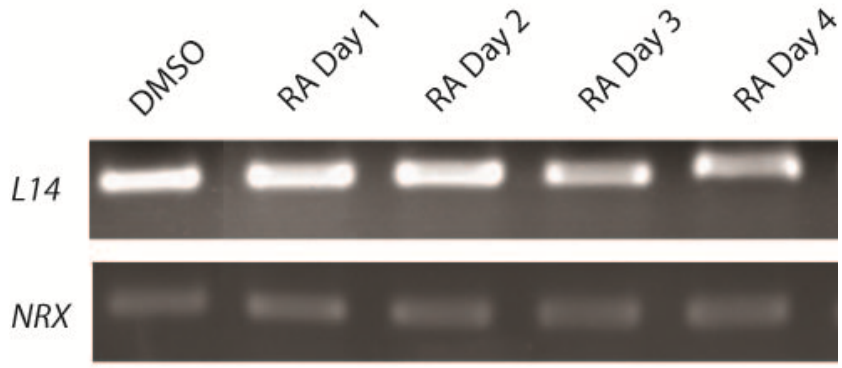
DMSO
RA Day 1
RA Day 2
RA Day 3
RA Day 4
L14
NRX

B

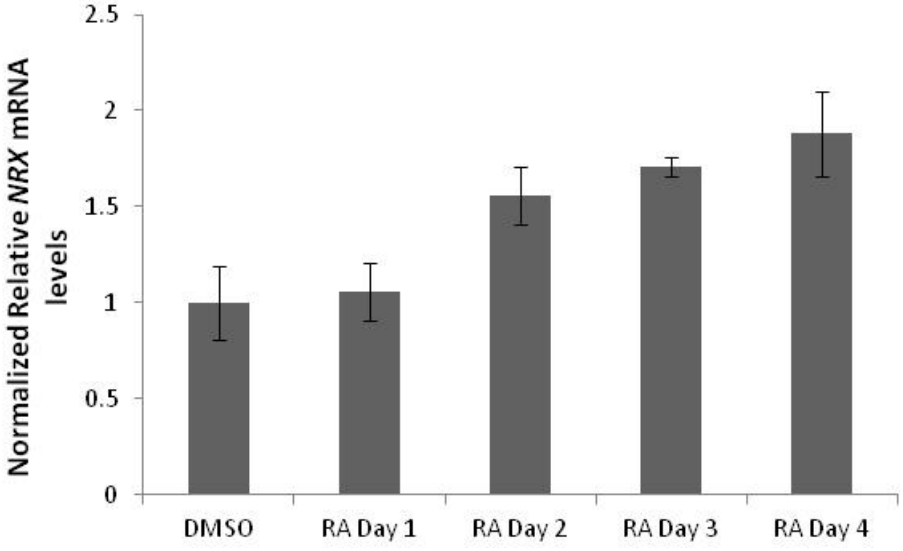
Normalized Relative NRX mRNA levels
2.5
2
1.5
1
0.5
0
DMSO
RA Day 1
RA Day 2
RA Day 3
RA Day 4

Unlike *Gata6* (Fig. 3.3G), these results strongly suggest that *NRX* is not RA-responsive.

3.6 NRX protein expression profile remains constant after RA treatment

To complete my analysis of NRX it was necessary to determine if RA affected the steady state levels of the protein. Total protein lysates from cells treated with DMSO or RA for 1 to 4 days were separated, transferred to membranes and then probed with either an NRX antibody or an antibody for β-actin, the latter protein serving as a loading control. Results show NRX bands, of the expected molecular mass, in DMSO and RA-treated cells (Fig. 3.6A). Furthermore, densitometry analysis showed no significant change in NRX protein levels between treatments (Fig. 3.6B). These results, like those for Dvl, show that NRX is expressed in undifferentiated F9 cells as well as in PrE cells induced by RA. Thus, if NRX can regulate Dvl and keep F9 cells in an undifferentiated state when Wnt ligands are absent, then the apparent inability of RA to alter the steady-state levels of either of these proteins would suggest that some other post-translational mechanism of regulation must be in effect.

3.7 Interaction between NRX and Dvl-2 is redox regulated

Given that F9 cells treated with RA demonstrate increased *Wnt6* expression and differentiate into PrE and that this increase is accompanied by a concomitant increase in

Figure 3.6 NRX protein levels are not RA responsive. F9 cells were treated with DMSO or RA (10^{-7} M) for 1 to 4 days and protein lysates were collected and used for immunoblot analysis. (A) Immunoblot showing relative NRX levels after cells were treated with DMSO or RA. NRX protein levels were not affected by RA treatment. (B) Densitometry results show no significant change in NRX protein levels in DMSO or RA treated cells. Densitometry was calculated by comparing the NRX/β-actin ratio of each treatment to the same ratio in the vehicle control treatment. Asterisks denote significant difference ($p \leq 0.05$). Data is representative as the mean and standard error of three independent experiments.

A

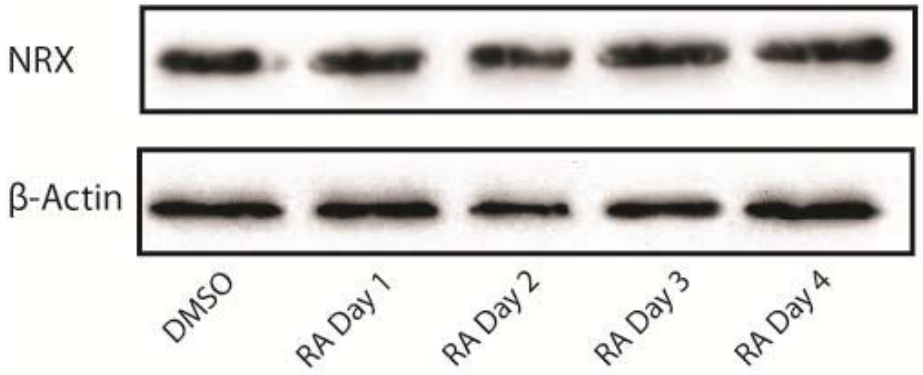
NRX
β-Actin
DMSO
RA Day 1
RA Day 2
RA Day 3
RA Day 4

B

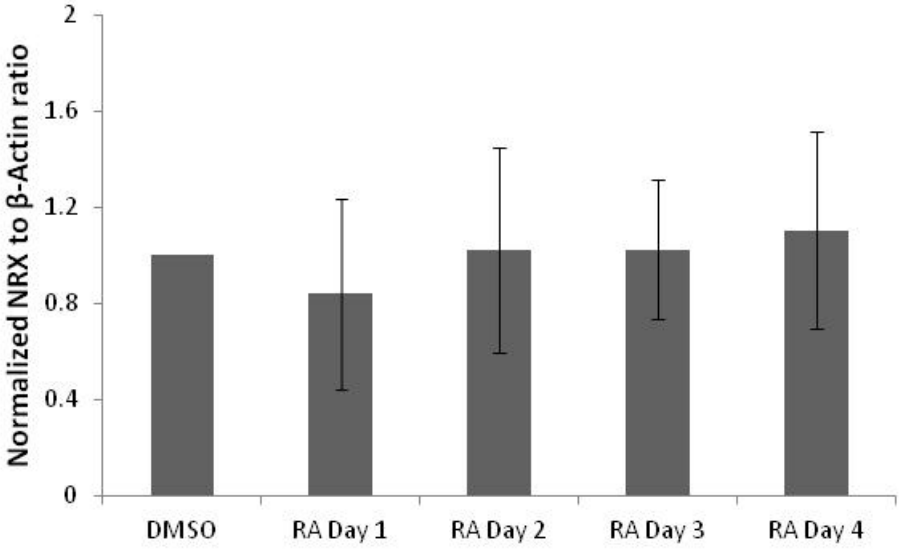
Normalized NRX to β-Actin ratio
2
1.6
1.2
0.8
0.4
0
DMSO
RA Day 1
RA Day 2
RA Day 3
RA Day 4

the levels of ROS, and treating F9 cells with H_2O_2 also induces differentiation [18], it is tempting to speculate that the redox state of the cell impacts on canonical Wnt signaling required for differentiation. The studies with NIH3T3 cells, showing that the interaction between NRX and Dvl-1 is redox regulated, also lends support to this model, implicating ROS signaling crosstalk with the Wnt pathway. Since NRX and Dvl are not responsive to RA in F9 cells, the possibility therefore exists that the increase in ROS following RA treatment plays a post-translational role in regulating the interaction between NRX and Dvl. If this is the case, then the ROS might be expected to cause disulfide bridge formation in the CXXC site of NRX, altering its conformation and affecting its ability to interact with Dvl. If my hypothesis is correct, then I expect to find NRX bound to Dvl in untreated F9 cells. Likewise, I predict that NRX would dissociate from Dvl when F9 cells are exposed to increasing levels of ROS. As noted above, Dvl-2 is the most abundant of the Dvl isoforms in F9 cells. I thus chose to further examine the relationship between NRX and Dvl-2.

To test my hypothesis, F9 cells were cultured and treated with H_2O_2, DTT (a strong reducing agent) or left untreated. Whole cell lysates were isolated and immunoprecipitated using an anti-Dvl-2 antibody to test the interaction between Dvl-2 and NRX. Normal mouse IgG was used as a negative control to assess for non-specific binding (Fig. 3.7A Lane 1). Following immunoprecipitation, immunoblot analysis revealed that in untreated cells, NRX binds to Dvl-2 (Lane 2). This interaction between NRX and Dvl-2 increased under strong reducing conditions (Lane 3), while under oxidizing conditions it appeared that the level of NRX bound to Dvl-2 decreased (Lane 4). Densitometry analysis was then used to assess the relative amounts of NRX-bound to

Figure 3.7 The interaction between NRX and Dvl-2 in F9 cells is redox-dependent. Cells were either untreated, or treated with DTT (1 mM) or H_2O_2 (1 mM) for 15 min and protein lysates were collected. Protein complexes were immunoprecipitated with an anti-Dvl-2 antibody or with an IgG Normal Mouse as a control. (A) Immunoblot results show that compared to controls, NRX levels pulled down with Dvl-2 decrease when cells were treated with H_2O_2. In converse, cells treated with DTT show that more NRX was pulled down in the Dvl-2 complex. (B) Densitometry analysis confirmed that NRX protein levels were significantly less in H_2O_2-treated cells compared to those treated with DTT. Densitometry was calculated by comparing the NRX/Dvl-2 ratio of DTT and H_2O_2 treatments to the same ratio in the untreated control. Asterisks denote significant difference ($p \leq 0.05$). Data is representative as the mean and standard error of three independent experiments.

A

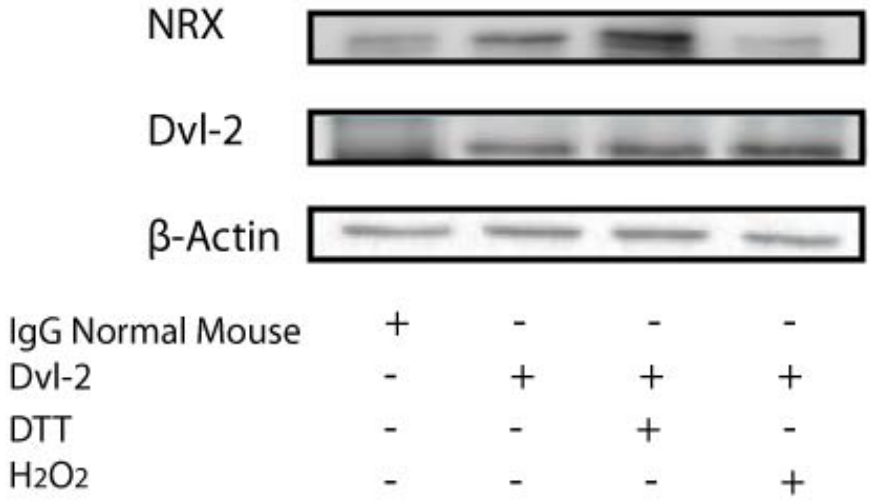
NRX
Dvl-2
β-Actin
IgG Normal Mouse + - - -
Dvl-2 - + + +
DTT - - + -
H2O2 - - - +

B

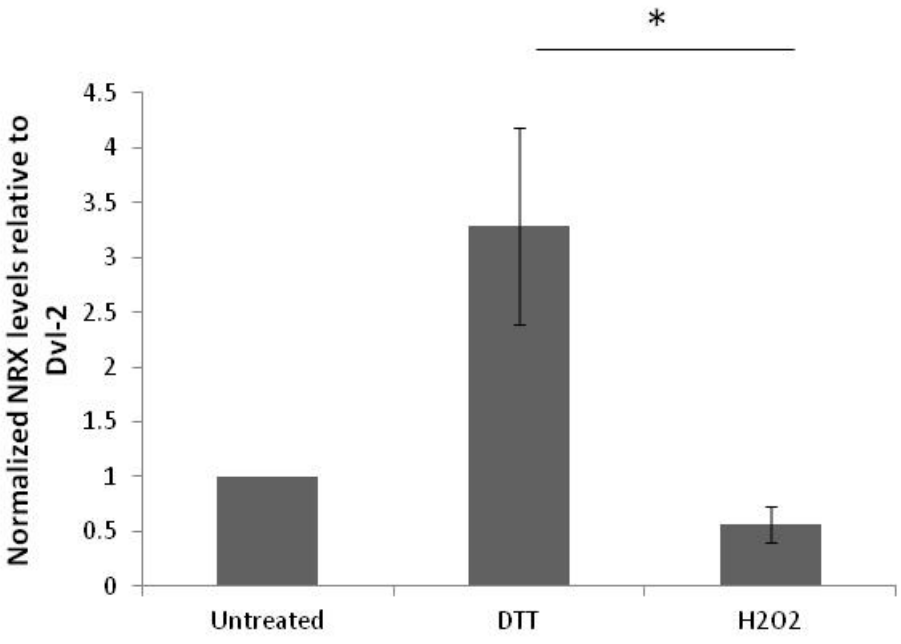
*
Normalized NRX levels relative to Dvl-2
4.5
4
3.5
3
2.5
2
1.5
1
0.5
0
Untreated
DTT
H2O2

Dvl-2 under the different treatment regimes (Fig. 3.7B). The data represent NRX bound to immunoprecipitated Dvl-2, and normalized to the levels of Dvl-2 pulled down. There was a significant difference in the amount of NRX bound to Dvl-2 when cells were subjected to DTT compared to H_2O_2 treatment ($p=0.03$). While there were differences in the amount of NRX bound to Dvl-2 in DTT and H_2O_2, compared to that in untreated cells, these differences were not significant ($p=0.06$ and $p=0.80$ respectively). These results provide evidence that NRX interacts with Dvl-2 in F9 cells, and furthermore that this relationship is redox dependent.

3.8 NRX knockdown differentiates F9 cells to PrE

NRX inhibits Dvl in the absence of Wnt, causing degradation of β-catenin and thus preventing the interaction between β-catenin and TCF-LEF [31]. In F9 cells, NRX is bound to Dvl-2 and the increase in ROS, following RA-induced Wnt activation, may affect the redox interaction between NRX and Dvl-2. That said, if ROS induce a conformational change in NRX this would free up a pool of Dvl, thereby priming it to be recruited to the plasma membrane if and when a Wnt ligand presents itself to a Fzd receptor. On the other hand, freeing up Dvl may be sufficient to activate the pathway in the absence of Wnt, as evident from studies showing the overexpression of Dvl alone upsets the stoichiometry of the Wnt pathway leading to activation [37]. In any event, the end result would be the accumulation of β-catenin, its translocation into the nucleus and its subsequent interaction with TCF-LEF to impart changes in gene expression necessary for PrE differentiation. If this premise is true, then knocking down NRX should release

the inhibition of Dvl and, in the absence of RA, free up enough Dvl to activate β-catenin-dependent gene expression needed for cells to differentiate into PrE.

To address my hypothesis, NRX was knocked down by transfecting F9 cells with a shRNA that specifically targets NRX. Changes in morphology were then evaluated using phase contrast microscopy. F9 cells were also transfected with the pRS empty vector plasmid (pRS-EV) as a control. Morphologically, cells transfected with pRS-EV and those treated with DMSO are similar and show cells growing in compact bodies, reminiscent of undifferentiated cells (Fig. 3.8A). Cells transfected with sh-*NRX* were elongated and flattened and showed changes in morphology including protrusions that differed from DMSO or pRS-EV-transfected cells. Interestingly, the sh-*NRX* morphology appeared similar to that caused by RA, suggesting the NRX knockdown was able to differentiate cells into PrE (Fig. 3.8A).

To test whether or not the NRX knockdown had induced cells to differentiate into PrE, protein lysates were collected for cells treated with DMSO or RA or transfected with pRS-EV or sh-*NRX*. Immunoblot analysis and the TROMA-1 antibody were used to detect the expression of cytokeratin intermediate filaments, a marker of PrE. An anti-NRX antibody was used to confirm the knockdown and β-actin was used to ensure equal amounts of protein were assayed between the different regimens. As expected, TROMA-1 levels appeared higher in RA treated cells compared to those treated with DMSO (Fig. 3.8B). TROMA-1 levels also appeared higher in cells transfected with sh-*NRX* compared to those transfected with pRS-EV (Fig. 3.8B). Densitometry data confirmed these results,

Figure 3.8 NRX knockdown increased endo-A cytokeratin levels indicative of extraembryonic endoderm differentiation. F9 cells transfected with sh-*NRX* or pRS-EV or treated with DMSO or RA (10^{-7} M), as controls, were examined morphologically or processed for immunoblot analysis using the TROMA-1 antibody to detect endo-A intermediate filaments. (A) F9 cells transfected with pRS-EV are morphologically similar to cells treated with DMSO, appearing in tightly compact groups reminiscent of undifferentiated cells. In contrast, F9 cells transfected with sh-*NRX* show a flattened, more elongated morphology, comparable to RA-treated differentiated primitive endoderm cells. (B) Immunoblot analysis with the TROMA-1 antibody indicates that endo-A intermediate filaments were present in cells transfected with sh-*NRX,* but not in cells transfected with the empty vector. This increase was seen in the RA-treated positive controls, but not in the DMSO negative control. Antibodies to NRX confirmed the efficiency of the NRX knockdown, while antibodies to β-actin was to ensure equal loading between samples. (C) Densitometry analysis confirmed that there was a significant increase in TROMA-1 positive signal when cells were transfected with sh-*NRX* or treated with RA compared to those transfected with pRS-EV or treated with DMSO, respectively. Densitometry was calculated by comparing the TROMA-1/β-actin ratio of RA and sh-*NRX* to the same ratio in the vehicle and pRS-EV control respectively. Asterisks denote significant difference ($p \leq 0.05$). Data is representative as the mean and standard error of three independent experiments. Scale bars = 20 μm.

A

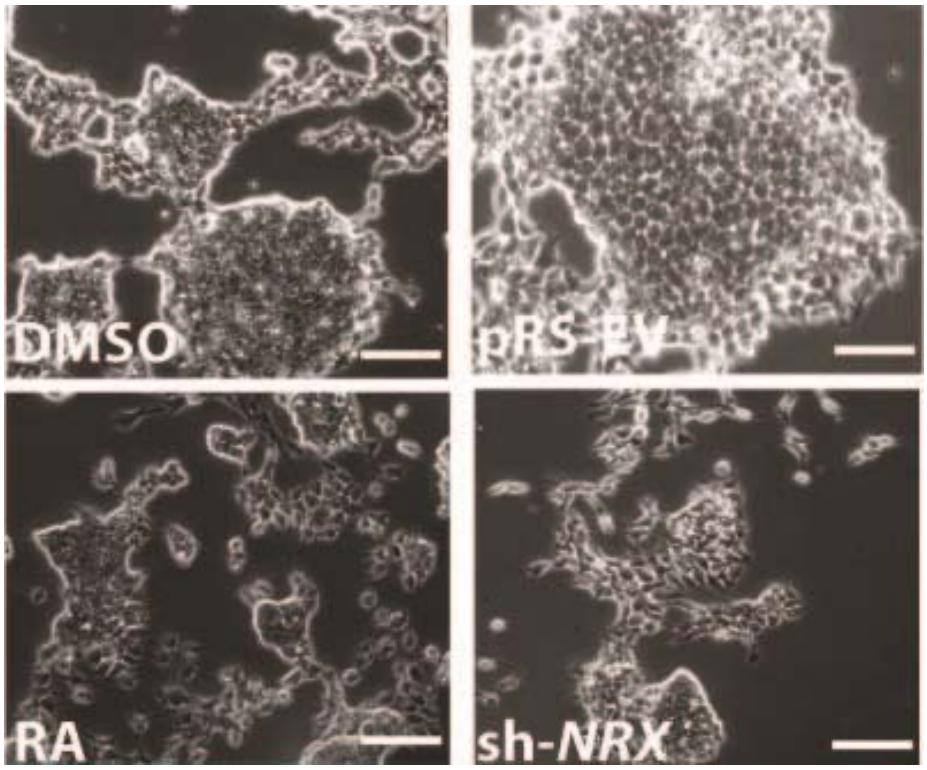
DMSO
pRS-EV
RA
sh-NRX

B

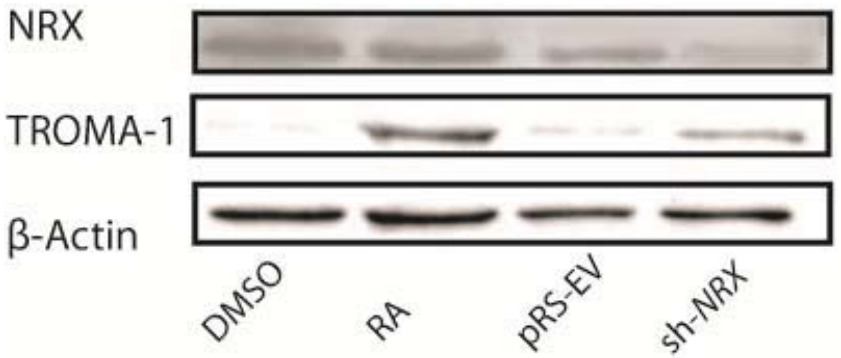
NRX
TROMA-1
β-Actin
DMSO
RA
pRS-EV
sh-NRX

C

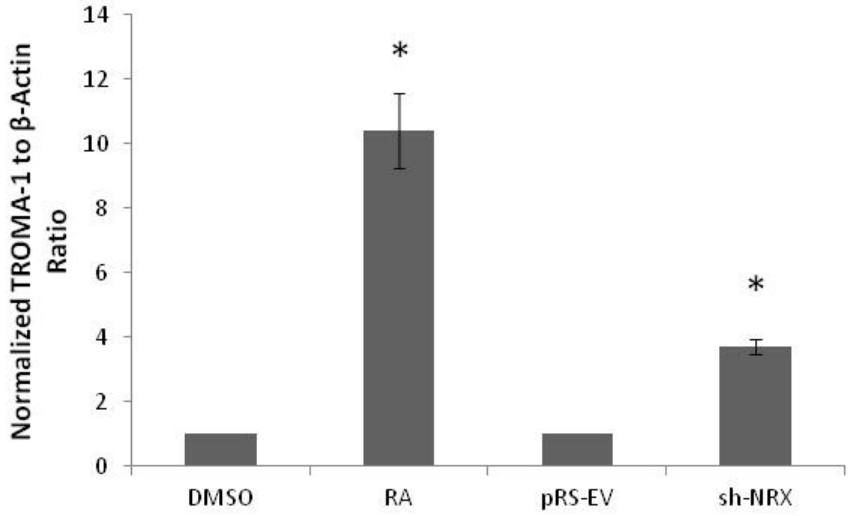
Normalized TROMA-1 to β-Actin Ratio
14
12
10
8
6
4
2
0
*
*
DMSO
RA
pRS-EV
sh-NRX

and showed there was a significant increase in TROMA-1 levels in RA-treated cells compared to those seen in DMSO treatments (Fig 3.8C). These levels were comparable to the significant increase seen in TROMA-1 levels resulting from the NRX knockdown (Fig. 3.8C). Thus, in the absence of RA, NRX knockdown in F9 cells is sufficient to induce PrE.

3.9 NRX knockdown plus db-cAMP differentiates F9 cells to PE

Since knocking down NRX caused cells to differentiate into PrE, the question remained as to whether or not F9 cells deficient in NRX were competent, under the right conditions, to differentiate into PE. To test this notion, sh-*NRX* transfected cells were treated with db-cAMP. As a control, cells were transfected with pRS-EV and treated with db-cAMP. Morphologically, cells transfected with pRS-EV and treated with db-cAMP were indistinguishable from those treated with DMSO. Both treatments showed cells growing in compact bodies, reminiscent of undifferentiated cells (Fig 3.9A). In contrast, cells transfected with sh-*NRX* and treated with db-cAMP were morphologically similar to those treated with RA and db-cAMP. sh-*NRX*-transfected and db-cAMP-treated cells exhibited the hallmark features of PE cells that had been induced by RA and db-cAMP, including extended cell protrusions and a refractile appearance (Fig. 3.9A).

Next, mRNA was isolated and converted into cDNA for a qRT-PCR analysis to confirm that the morphological changes resulting from the NRX knockdown were associated with decreased levels of NRX expression. qRT-PCR results show cells

Figure 3.9 F9 cells transfected with sh-NRX and treated with db-cAMP form parietal endoderm. Total RNA from F9 cells transfected with pRS-EV or sh-*NRX*, or transfected with pRS-EV or sh-*NRX* and then treated with db-cAMP was isolated, reverse transcribed into first strand cDNA, and used as template for PCR analysis with primers designed to *NRX, TM,* and *L14* (control). RNA was also collected from cells treated with DMSO, RA (10^{-7} M), or RA and db-cAMP (0.05 mM). (A) F9 cells transfected with pRS-EV and treated with db-cAMP grow in tightly compact groups, similar to DMSO-treated cells. F9 cells transfected with sh-*NRX* and then treated with db-cAMP are morphologically different from controls, having increased cell protrusions and a refractile appearance. This morphology is reminiscent of cells treated with RA and db-cAMP. (B) qRT-PCR analysis for *NRX* confirms that there was a significant decrease in the level of *NRX* in cells transfected with sh-*NRX* and in cells transfected with sh-*NRX* and treated with db-cAMP. (C) qRT-PCR results show *NRX* levels at the exponential (cycle 25) and the plateau (cycle 40) phases. Note that during the exponential phase a *NRX* amplicon is not seen in cells transfected with sh-*NRX* or in those transfected with sh-*NRX* and then treated with db-cAMP. An amplicon, however, was seen at the plateau phase. (D) qRT-PCR indicates that compared to the empty vector control, there was a significant increase in *TM* in cells transfected with sh-*NRX* and treated with db-cAMP. The same is true for RA and db-cAMP-treated cells compared to the DMSO control. (E) The *TM* signal at the exponential (cycle 29) phase from cells transfected with sh-*NRX* and then treated with db-cAMP is similar to the signal seen from cells treated with RA and db-cAMP. The increase in *TM* expression is seen at the plateau phase under all treatment regimes. For qRT-PCR analysis, the expression level of *NRX* and *TM* was normalized to *L14* and

compared to the vehicle or pRS-EV control. Asterisks denote significant difference ($p \leq 0.05$). Data is representative as the mean and standard error of three independent experiments. Scale bars = 20 μm.

A

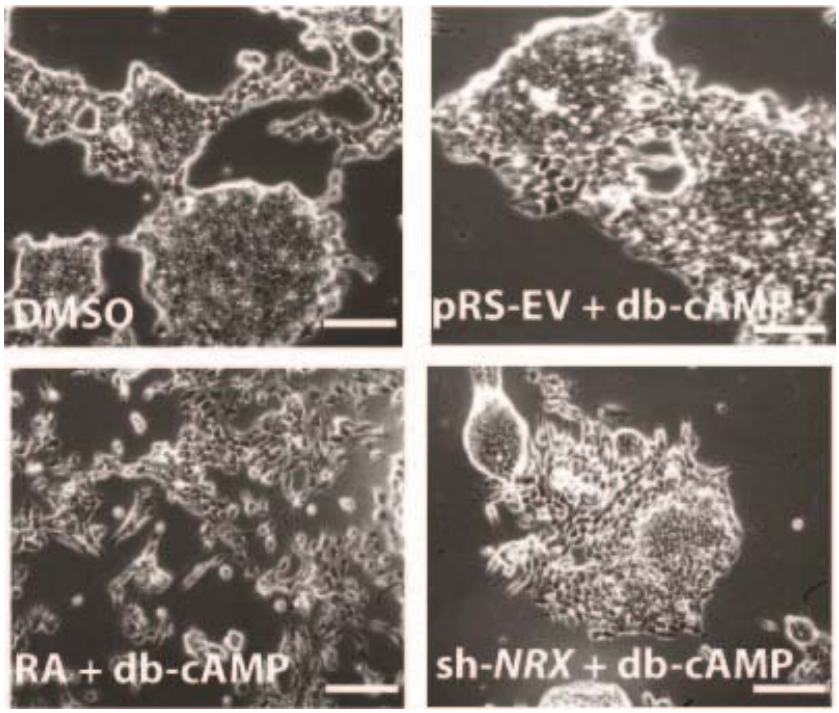
DMSO
pRS-EV + db-cAMP
RA + db-cAMP
sh-NRX + db-cAMP

B

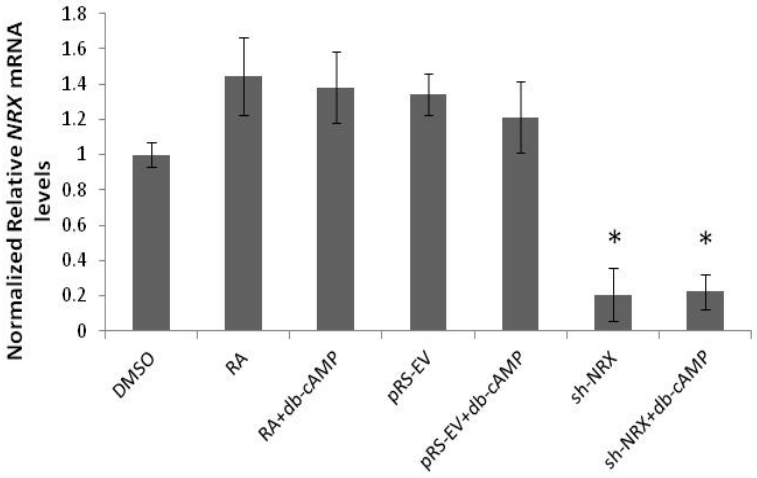
Normalized Relative NRX mRNA levels
1.8
1.6
1.4
1.2
1
0.8
0.6
0.4
0.2
0
*
*
DMSO
RA
RA+db-cAMP
pRS-EV
pRS-EV+db-cAMP
sh-NRX
sh-NRX+db-cAMP

C

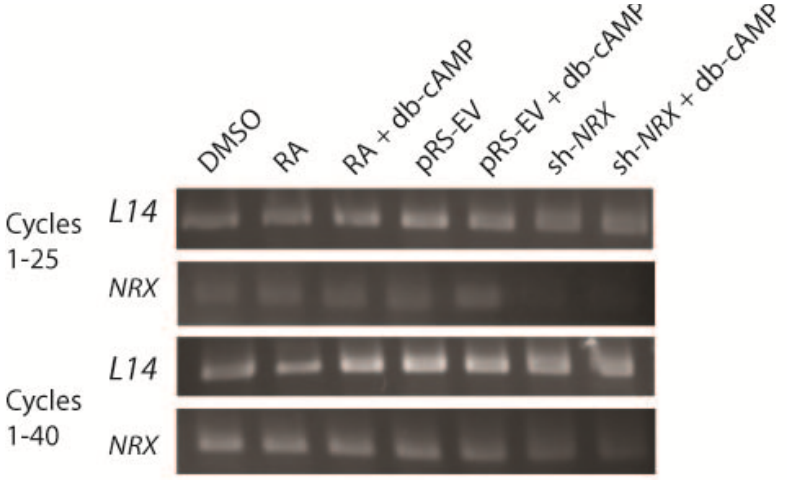
DMSO
RA
RA + db-cAMP
pRS-EV
pRS-EV + db-cAMP
sh-NRX
sh-NRX + db-cAMP
Cycles 1-25
L14
NRX
Cycles 1-40
L14
NRX

D

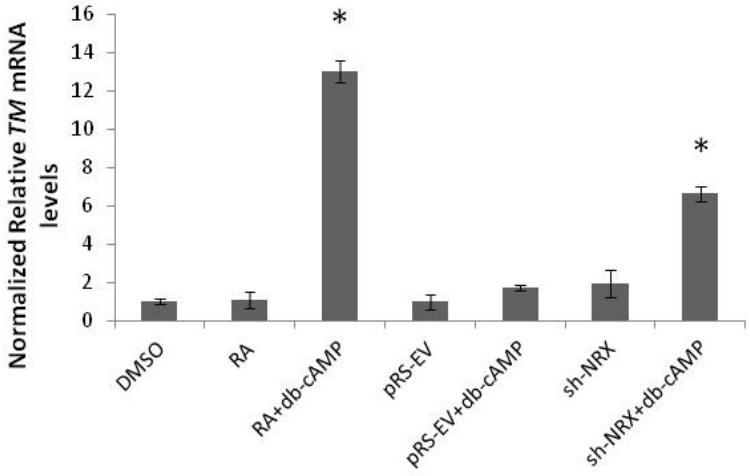
Normalized Relative TM mRNA levels
16
14
12
10
8
6
4
2
0
*
*
DMSO
RA
RA+db-cAMP
pRS-EV
pRS-EV+db-cAMP
sh-NRX
sh-NRX+db-cAMP

E

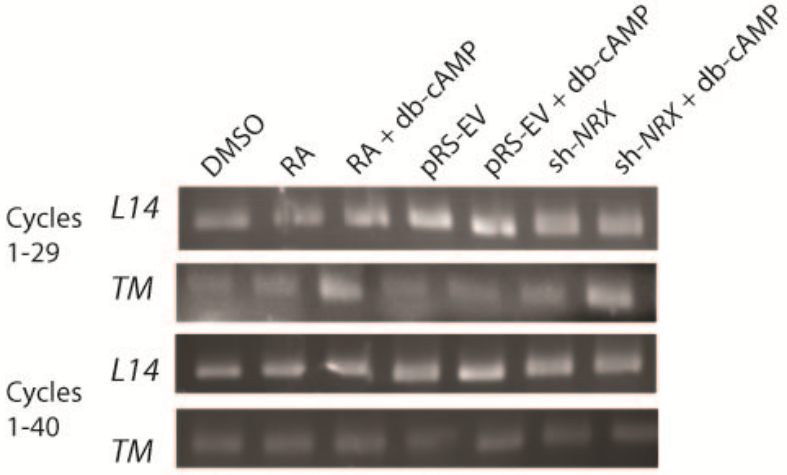
DMSO
RA
RA + db-cAMP
pRS-EV
pRS-EV + db-cAMP
sh-NRX
sh-NRX + db-cAMP
Cycles 1-29
L14
TM
Cycles 1-40
L14
TM

transfected with sh-*NRX* had a significant decrease in *NRX* levels compared to cells transfected with the pRS-EV (Fig. 3.9B). To account for the fact that the knockdown was not 100% efficient, qRT-PCR samples were run in duplicate, stopping one set at the cycle threshold, the number of cycles at which the dsDNA fluoresces. The second set was run until completion, the full 40 cycles. Samples from both groups were electrophoresed on agarose gels and images collected. These results show that after 25 cycles, the cycle threshold, *NRX* amplicons were not evident in cells transfected with sh-*NRX* or in those transfected sh-*NRX* and treated with db-cAMP; however, transcript levels of *NRX* after 40 cycles, the endpoint, show similar *NRX* transcript levels in all treatments (Fig. 3.9C). Therefore, visualising *NRX* at its cycle threshold, using electrophoresis and qRT-PCR data, indicates the efficiency of the knockdown.

The efficiency of the *NRX* knockdown was confirmed, and the morphological changes seen due to the knockdown suggested cells had differentiated to PE. To confirm the latter, qRT-PCR was used with primers designed against the PE marker *TM*. Relative to their respective controls, there was a significant increase in the *TM* expression in cells treated with RA and db-cAMP and in cells transfected with sh-*NRX* and then subsequently treated with db-cAMP (Fig. 3.9D). Samples were assayed at the cycle threshold (cycle 29), and at the 40 cycle endpoint (Fig. 3.9E). After 29 cycles, treatments with DMSO or RA alone had no effect on *TM* expression. In contrast, *TM* amplicons were seen in the RA and db-cAMP positive control. *TM* amplicons were not detected in cells transfected with pRS-EV alone, or pRS-EV and then treated with db-cAMP. Finally, transfecting cells with sh-*NRX* had no affect on up-regulating the *TM* gene, but adding db-cAMP following transfection resulted in increased *TM* expression. That transcript

levels of *TM* after 40 cycles appear similar in all treatments highlights the importance of validating qRT-PCR data at the cycle threshold of the gene of interest.

Together, these results confirm that the knockdown of NRX alone is not sufficient to induce F9 cells to differentiate as PE. Likewise, transfecting cells with the pRS-EV construct and them treating with db-cAMP does not induce cells to PE. Rather, in a manner that mimics the induction of PE by RA and db-cAMP, the NRX knockdown is sufficient to induce cells to differentiate as PrE that is competent to differentiate into PE when challenged with db-cAMP.

Chapter 4

4 Discussion

Wnt signaling plays numerous roles in vertebrate and invertebrate development and if the molecular changes seen in the *in vitro* F9 model are *bona fide* and directly recapitulate those *in vivo*, then we can infer that the redox regulation of the Wnt signaling pathway is responsible for specifying a select group of ICM cells to differentiate as PrE. In addition to canonical Wnt/β-catenin signaling, two other pathways involving Wnt include the planar cell polarity (PCP) and the Wnt/Ca^{2+} pathways. The PCP pathway is important in gastrulation as it mediates changes in the cytoskeleton affecting cell morphology. For PCP signaling, Wnt works through Fzd and Dvl to act on the Rho-Rac-JNK pathway, independent of β-catenin [12]. PCP signaling also plays a role in the differentiation of F9 cells into PrE [38], but investigating this pathway in addition to canonical Wnt signaling was beyond the scope of my thesis. Likewise, the third and least understood Wnt pathway involving Wnt/Ca^{2+} was not investigated, and to date only one paper has been reported to indirectly implicate the involvement of this pathway in F9 cell differentiation [39]. Nevertheless, the fact that the Wnt/Ca^{2+} pathway signals through Fzd, G-proteins, calcium/calmodulin-dependent kinase II and protein kinase C to trigger downstream targets for cellular polarity and adhesion affecting body axis specification during embryogenesis [40], it may be imprudent to dismiss it in having a role earlier in mouse development. Given the three known Wnt pathways, the focus of my research was on redox regulation pertaining only to Wnt/β-catenin signaling.

A growing body of evidence, including some provided by this work, indicates that Wnt/β-catenin signaling is redox regulated and that ROS play a significant role in these early events. My study used the F9 teratocarcinoma cell line, which differentiates into PrE upon the addition of RA, and PE following treatment with RA and db-cAMP. The addition of RA is accompanied by increased ROS levels, which are necessary to facilitate the differentiation to PrE [18]. Furthermore, when F9 cells are treated with RA, data indicates that the accompanied increase in ROS signaling is necessary to regulate components of the Wnt pathway, in particular NRX and Dvl.

Our working model proposes that in the absence of Wnt, NRX binds Dvl, thereby preventing the latter from destabilizing the β-catenin destruction complex. RA causes changes in gene expression, including the upregulation of *Wnt6,* and an increase in ROS which results in the dissociation of Dvl from NRX. Dvl is now primed and is recruited to the plasma membrane following binding of the Wnt ligand to its Fzd receptor and LRP-5/6 co-receptor. The subsequent increase in cytoplasmic β-catenin, resulting from the disassembly of its GSK-3β, Axin and APC destruction complex, leads to its translocation into the nucleus where together with TCF-LEF, it can impart changes in gene expression necessary for PrE differentiation [16, 18]. This model is of course in its simplest form and one might question why the cell needs the negative regulation of NRX on Dvl when the Wnt ligand is absent. Although there are many plausible explanations, the one we favour involves a failsafe mechanism, where this negative regulation prevents aberrant activation of the Wnt pathway in the absence of the Wnt ligand. This may also explain why the pathway can be activated by overexpressing Dvl [31].

4.1 Increase in ROS is necessary for ExE differentiation

RA is a morphogen that acts via nuclear receptors to exert its effects on F9 cells to induce PrE [41]. Treatment of F9 cells with RA and db-cAMP further differentiates cells from PrE to PE. This differentiation of F9 cells to PrE and PE is accompanied by reduced cell proliferation, morphological changes, and transcriptional activation of several genes including cytokeratin endo-A and tissue plasminogen activator [42]. Recently, we found that this RA-induced differentiation to PrE in F9 cells is accompanied by an increase in the levels of ROS. Furthermore, it was shown that RA signaling and the subsequent increase in the levels of ROS converge on the canonical Wnt-β-catenin pathway, which incidentally is required to induce PrE [18]. My study confirmed that RA and ROS converge in F9 cells to induce PrE by detection of cytokeratin endo-A in RA and H_2O_2 treated cells. Likewise, my results corroborate those showing that *TM* is expressed when RA-treated F9 cells are exposed to compounds that elevate intracellular cyclic AMP levels indicating differentiation to PE [14]. Two very significant findings derived from my study pertained to PE, and its ability to form in the absence of RA, when F9 cells are either treated with H_2O_2 and db-cAMP or when NRX depleted F9 cells are treated with db-cAMP. These studies highlight the importance of redox signaling in the regulation of cellular processes associated with differentiation.

The regulation of redox signaling in cells is imperative as high ROS levels may lead to cellular damage [21]. The importance of redox signaling with respect to differentiation has recently attracted much attention. For instance, Yanes *et al.* (2010) showed that the amounts of oxidative and reducing agents present in embryonic stem

cells are inversely related and important in mediating embryonic cell fate [43]. Furthermore, my study has revealed that exposure to reducing agents like ascorbic acid (Vitamin C) or NAC, significantly reduces the ability of F9 cells to differentiate in the presence of RA, and this is consistent with the notion that signaling pathways involved in differentiation are redox regulated. That low levels of Vitamin C (0.1 mM) were not sufficient to significantly reduce the ability of F9 cells to differentiate in the presence of RA may be explained by the fact that these antioxidant levels along with the increase of ROS following RA-induction were not high enough to upset the redox regulation, and while differentiation is hindered, it is not significantly affected. Higher concentrations of Vitamin C (0.5 mM) and NAC (1 mM and 2 mM), however, were sufficient to overcome the increase in ROS levels following RA treatment and therefore were able to retard differentiation. While intracellular ROS levels were unaccounted for in this study, the idea is consistent with previous reports indicating that the intracellular oxidation state regulates cell differentiation [43].

4.2 Dvl and NRX are not RA responsive in F9 cells

Treatment of F9 cells with RA, and subsequent increase in ROS levels activates Wnt signaling, specifically Wnt6 in F9 cells, causing differentiation to PrE [16]. This increase in *Wnt6* is caused by upregulation of the RA responsive genes, Gata6 and FoxA2; *Gata6* is a direct target gene of RA signaling and *FoxA2* a target gene of Gata6 [12]. Wnt6 in F9 cells is necessary for PrE differentiation as the binding of Wnt to its receptors cause Dvl to be recruited to the plasma membrane. Here, Dvl acts to inhibit the

destruction complex allowing β-catenin to accumulate and bind to TCF-LEF in the nucleus to activate genes necessary for PrE differentiation. Since RA causes increased levels of Gata6 and FoxA2, which in turn activate Wnt signaling, and since Dvl is an important regulator of the Wnt signaling pathway, I examined the possibility of Dvl regulation by RA induction. Studies by Lee *et al.* (2008) on Dvl in F9 cells indicate all three isoforms are present and show great importance in Wnt signaling as the loss of Dvl decreases the canonical response to Wnt by impacting TCF-LEF response [34]. My study confirms the presence of all three Dvl isoforms in F9 cells, and demonstrated that upon RA treatment the relative levels of Dvl remain constant in comparison to vehicle treated cells. Even though Dvl is not RA responsive, the presence of Dvl-1, Dvl-2, and Dvl-3 in both undifferentiated and differentiated cells indicates its importance to F9 cells.

Interestingly, Funato *et al.* (2006) reported that Dvl binds to NRX in the Wnt/β-catenin pathway. Since NRX is a binding partner of Dvl, it was thought that if Dvl is not regulated by RA then a possible candidate is NRX. My study is the first to look at the role of NRX in F9 cells and its affect on differentiation to ExE. While I found that NRX is present in F9 cells, the expression of NRX remained constant following RA treatment compared to vehicle treated cells. While neither NRX nor Dvl show response to RA treatment, their steady-state levels would indicate that they are regulated by other post-translational mechanisms.

4.3 Redox regulated interaction between NRX and Dvl-2

The results of this study clearly show that the levels of NRX and Dvl mRNA or protein in F9 cells were not affected by RA. However, their ability to interact under oxidizing and reducing conditions, which in the case of the former would mimic the ROS burst that accompanies differentiation, was examined in detail. Previous reports have shown that NRX is redox-regulated as it contains an amino acid sequence with a redox active site, CXXC. Under oxidizing conditions, the thiol functional group on the two cysteine residues, in the CXXC motif, form a disulfide bridge capable of changing protein function or protein-protein interactions [27, 31]. Given this evidence, it seemed likely that ROS would affect the redox active site on NRX in F9 cells, thereby altering its conformation and ability to interact with other proteins [18]. Interestingly, immunoprecipitation studies and mass spectrometry of NIH3T3 murine fibroblast cells have been used to identify NRX as a Dvl-1 binding protein [31]. Since NRX contains a redox active site, the authors of this study tested the effects of oxidizing and reducing conditions on Dvl-1-NRX binding. Their data clearly show that NRX-bound Dvl-1 increases under reducing conditions, and decreases under oxidizing conditions [31], thereby reinforcing the idea that NRX is a redox sensitive protein.

The interaction between NRX and Dvl was also shown for F9 cells in my study. Here, the relationship between NRX and Dvl-2 was observed using co-immunoprecipitation analysis. Using this technique I was able to show that the amount of NRX-bound to Dvl-2 increased under reducing conditions; conversely the amount of NRX-bound to Dvl-2 decreased under oxidizing conditions.

Given these results it seems logical to predict that the burst of ROS that occurs in F9 cells treated with RA [18] would impact on the ability of NRX to bind Dvl-2, freeing up the latter to transduce the Wnt signal when the ligand is present.

4.4 NRX inhibits Wnt signaling induced ExE differentiation

Given the accompanied increase in ROS levels after RA induction that activates a canonical Wnt pathway, and that NRX and Dvl-2 show a redox dependant relationship, the idea must be put forth that NRX is an important regulator of Wnt signaling. As described earlier, in the presence of a canonical Wnt, Dvl is recruited to the plasma membrane and the levels of cytoplasmic β-catenin increase by virtue of the fact that its destruction complex (involving GSK-3β, Axin and APC) can no longer function. The β-catenin pool in the cytoplasm increases and some translocates into the nucleus where, with TCF-LEF, the complex imparts changes to Wnt target genes. Funato *et al.* (2006) examined the ability of NRX to induce activation of TCF using a luciferase reporter gene assay. Dvl overexpression led to increased levels of TCF activity, while the expression of TCF was completely suppressed by co-expression of NRX. Furthermore, TCF activity was upregulated in cells expressing an *NRX* RNAi [31]. In F9 cells, the nuclear accumulation of β-catenin and its interaction with TCF-LEF is obligatory for PrE differentiation [41]. Although my study did not utilize a reporter assay, the NRX knockdown did result in a significant increase in the level of TROMA-1 staining on immunoblots, reminiscent of RA-induced differentiation. Taken together, this demonstrates that the knockdown of NRX alone is sufficient to induce differentiation.

Furthermore, knocking down NRX and increasing cAMP levels in the absence of RA, led to a significant increase in *TM*, indicating the cells were competent and had differentiated to PE. Thus given my data and the evidence from the literature, I propose that in the absence of NRX, Dvl is not inhibited. In this free form, Dvl is thus recruited to the plasma membrane where it serves to prevent the destruction complex from targeting β-catenin for proteasomal degradation. If this prediction is correct, then Dvl should be seen at or near the plasma membrane; likewise, examining TOPFlash reporter activity in cells transfected with the sh-*NRX* would also corroborate my prediction.

4.5 Relationship of NRX and Nox point to future research in F9 cells

Overall, the data presented provide compelling evidence that NRX plays an important role as a negative regulator of Wnt signaling in F9 teratocarcinoma cells. In our model the redox regulation of NRX is imperative in controlling Wnt signaling, which would take into account the increase in the levels of ROS following RA treatment (Fig. 4.1). In this manner, the increase in ROS is predicted to modulate the conformation of NRX, thereby releasing Dvl and allowing it to participate in the transduction of the Wnt signal necessary for PrE differentiation. Although it is easy to envision that NRX serves as a failsafe mechanism to prevent aberrant Wnt signaling, the question remains as to the source of ROS. Candidates include the Nox family of ROS producing enzymes, consisting of Nox1-4 and Duox2, that are present in F9 cells [18]. In support of this idea our lab has shown that RA-induced differentiation is hindered when F9 cells are treated with the Nox inhibitor DPI [18]. This study also revealed that the *Nox1–4* and *Duox2*

genes are RA-responsive. Nox4 has been linked to cell proliferation, migration and stem cell differentiation [44, 45], and that the *Nox1* promoter is known to be regulated by Gata6, a master regulator of ExE [46]. Furthermore, studies using intestinal cells showed overexpressing NRX blocks Wnt-induced accumulation of β-catenin, however, overexpressing NRX and coexpressing Nox1 had the reverse effect [47]. Although these studies are encouraging and supportive, at present we do not know which of the Nox enzymes are responsible for producing the burst of ROS that is seen in F9 cells following exposure to RA.

Despite not knowing the source that produces the ROS in response to RA, it is important to note that the regulation of these levels in the cell is essential since high levels of ROS and aberrant Wnt signaling are frequently demonstrated in cancer cells [43]. This NRX related redox regulation could have significant implications in understanding Wnt-dependent carcinogenesis. Towards that end, this study not only provides insight into how extraembryonic endoderm differentiates in the mammalian embryo, but it also gives us a better understanding of the relationship between ROS and the aberrant activation of signal transduction pathways involved in human pathophysiology.

Figure 4.1 A model for the differentiation of extraembryonic endoderm in F9 cells. RA acts through binding to RA receptors and retinoid X receptors which efficiently bind RA-response elements in the promoter regions of target genes. RA induces the expression of Nox, leading to the production of intracellular H_2O_2. This increase in H_2O_2 levels cause NRX to form a disulfide bridge changing conformation and causing the release of bound Dvl-2. This in turn with binding of Wnt6 to the Fzd receptor causes Dvl-2 to be recruited to the plasma membrane where it acts to destabilize the destruction complex causing an increase of β-catenin in the cytosol, subsequent translocation to the nucleus where it binds to TCF-LEF to alter gene expression necessary for differentiation to extraembryonic endoderm.

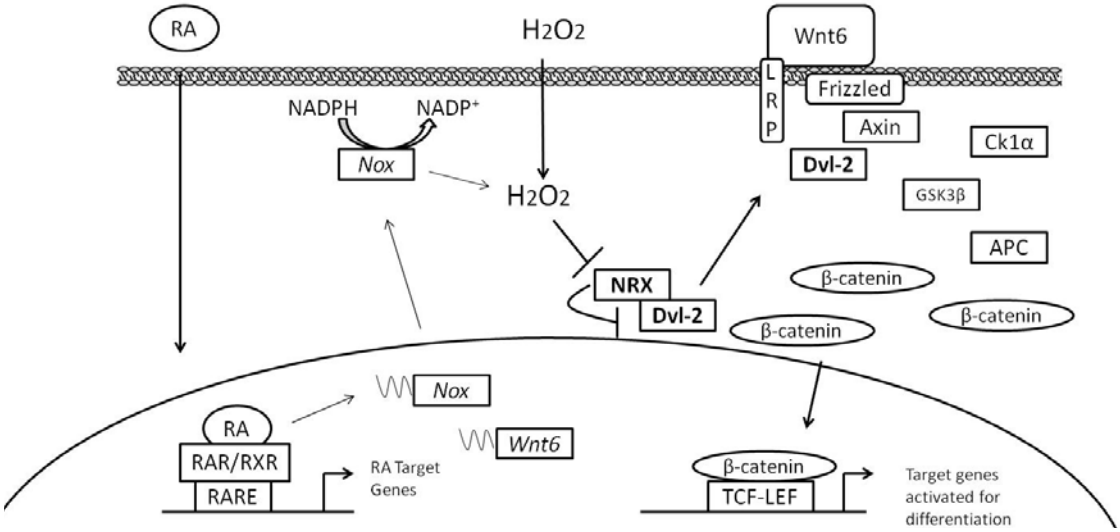
RA
H2O2
Wnt6
L
R
P
Frizzled
Axin
Ck1α
Dvl-2
GSK3β
APC
NADPH
NADP+
Nox
H2O2
NRX
Dvl-2
β-catenin
β-catenin
β-catenin
Nox
RA
RAR/RXR
RARE
RA Target
Genes
Wnt6
β-catenin
TCF-LEF
Target genes
activated for
differentiation

Literature Cited

1. Lu, C.C., J. Brennan, and E.J. Robertson, *From fertilization to gastrulation: axis formation in the mouse embryo.* Curr Opin Genet Dev, 2001. **11**(4): p. 384-92.

2. Niwa, H., et al., *Interaction between Oct3/4 and Cdx2 determines trophectoderm differentiation.* Cell, 2005. **123**(5): p. 917-29.

3. Tam, P.P. and D.A. Loebel, *Gene function in mouse embryogenesis: get set for gastrulation.* Nat Rev Genet, 2007. **8**(5): p. 368-81.

4. Imhof, B.A., et al., *Cell-cell interaction and polarity of epithelial cells: specific perturbation using a monoclonal antibody.* Cell, 1983. **35**(3 Pt 2): p. 667-75.

5. Boiani, M. and H.R. Scholer, *Regulatory networks in embryo-derived pluripotent stem cells.* Nat Rev Mol Cell Biol, 2005. **6**(11): p. 872-84.

6. Verheijen, M.H. and L.H. Defize, *Signals governing extraembryonic endoderm formation in the mouse: involvement of the type 1 parathyroid hormone-related peptide (PTHrP) receptor, p21Ras and cell adhesion molecules.* Int J Dev Biol, 1999. **43**(7): p. 711-21.

7. Strickland, S., K.K. Smith, and K.R. Marotti, *Hormonal induction of differentiation in teratocarcinoma stem cells: generation of parietal endoderm by retinoic acid and dibutyryl cAMP.* Cell, 1980. **21**(2): p. 347-55.

8. Berstine, E.G., et al., *Alkaline phosphatase activity in mouse teratoma.* Proc Natl Acad Sci U S A, 1973. **70**(12): p. 3899-903.

9. Strickland, S. and V. Mahdavi, *The induction of differentiation in teratocarcinoma stem cells by retinoic acid.* Cell, 1978. **15**(2): p. 393-403.

10. Gillespie, R.F. and L.J. Gudas, *Retinoic acid receptor isotype specificity in F9 teratocarcinoma stem cells results from the differential recruitment of coregulators to retinoic response elements.* J Biol Chem, 2007. **282**(46): p. 33421-34.

11. Su, D. and L.J. Gudas, *Gene expression profiling elucidates a specific role for RARgamma in the retinoic acid-induced differentiation of F9 teratocarcinoma stem cells.* Biochem Pharmacol, 2008. **75**(5): p. 1129-60.

12. Hwang, J.T. and G.M. Kelly, *GATA6 and FOXA2 Regulate Wnt6 Expression During Extraembryonic Endoderm Formation.* Stem Cells Dev, 2012. **21**(17): p. 3220-32.

13. Kemler, R., et al., *Reactivity of monoclonal antibodies against intermediate filament proteins during embryonic development.* J Embryol Exp Morphol, 1981. **64**: p. 45-60.

14. Weiler-Guettler, H., et al., *Thrombomodulin gene regulation by cAMP and retinoic acid in F9 embryonal carcinoma cells.* Proc Natl Acad Sci U S A, 1992. **89**(6): p. 2155-9.

15. Moon, R.T., *Wnt/beta-catenin pathway.* Sci STKE, 2005. **2005**(271): p. cm1.

16. Krawetz, R. and G.M. Kelly, *Wnt6 induces the specification and epithelialization of F9 embryonal carcinoma cells to primitive endoderm.* Cell Signal, 2008. **20**(3): p. 506-17.

17. Stemmer, V., et al., *Snail promotes Wnt target gene expression and interacts with beta-catenin.* Oncogene, 2008. **27**(37): p. 5075-80.

18. Wen, J.W., J.T. Hwang, and G.M. Kelly, *Reactive oxygen species and Wnt signalling crosstalk patterns mouse extraembryonic endoderm.* Cell Signal, 2012. **24**(12): p. 2337-48.

19. Tochhawng, L., et al., *Redox regulation of cancer cell migration and invasion.* Mitochondrion, 2012. **Epub ahead of print**.

20. Hernandez-Garcia, D., et al., *Reactive oxygen species: A radical role in development?* Free Radic Biol Med. **49**(2): p. 130-43.

21. Allen, R.G. and M. Tresini, *Oxidative stress and gene regulation.* Free Radic Biol Med, 2000. **28**(3): p. 463-99.

22. Chae, H.Z., et al., *Cloning and sequencing of thiol-specific antioxidant from mammalian brain: alkyl hydroperoxide reductase and thiol-specific antioxidant define a large family of antioxidant enzymes.* Proc Natl Acad Sci U S A, 1994. **91**(15): p. 7017-21.

23. Covarrubias, L., et al., *Function of reactive oxygen species during animal development: passive or active?* Dev Biol, 2008. **320**(1): p. 1-11.

24. Saitoh, M., et al., *Mammalian thioredoxin is a direct inhibitor of apoptosis signal-regulating kinase (ASK) 1.* EMBO J, 1998. **17**(9): p. 2596-606.

25. Schieven, G.L., et al., *Reactive oxygen intermediates activate NF-kappa B in a tyrosine kinase-dependent mechanism and in combination with vanadate activate the p56lck and p59fyn tyrosine kinases in human lymphocytes.* Blood, 1993. **82**(4): p. 1212-20.

26. Kurooka, H., et al., *Cloning and characterization of the nucleoredoxin gene that encodes a novel nuclear protein related to thioredoxin.* Genomics, 1997. **39**(3): p. 331-9.

27. Paulsen, C.E. and K.S. Carroll, *Orchestrating redox signaling networks through regulatory cysteine switches.* ACS Chem Biol, 2010. **5**(1): p. 47-62.

28. Hirota, K., et al., *Nucleoredoxin, glutaredoxin, and thioredoxin differentially regulate NF-kappaB, AP-1, and CREB activation in HEK293 cells.* Biochem Biophys Res Commun, 2000. **274**(1): p. 177-82.

29. Funato, Y., et al., *Nucleoredoxin sustains Wnt/beta-catenin signaling by retaining a pool of inactive dishevelled protein.* Curr Biol, 2010. **20**(21): p. 1945-52.

30. Boles, M.K., et al., *Discovery of candidate disease genes in ENU-induced mouse mutants by large-scale sequencing, including a splice-site mutation in nucleoredoxin.* PLoS Genet, 2009. **5**(12): p. e1000759.

31. Funato, Y., et al., *The thioredoxin-related redox-regulating protein nucleoredoxin inhibits Wnt-beta-catenin signalling through dishevelled.* Nat Cell Biol, 2006. **8**(5): p. 501-8.

32. Strovel, E.T. and D.J. Sussman, *Transient overexpression of murine dishevelled genes results in apoptotic cell death.* Exp Cell Res, 1999. **253**(2): p. 637-48.

33. Etheridge, S.L., et al., *Murine dishevelled 3 functions in redundant pathways with dishevelled 1 and 2 in normal cardiac outflow tract, cochlea, and neural tube development.* PLoS Genet, 2008. **4**(11): p. e1000259.

34. Lee, Y.N., Y. Gao, and H.Y. Wang, *Differential mediation of the Wnt canonical pathway by mammalian Dishevelleds-1, -2, and -3.* Cell Signal, 2008. **20**(2): p. 443-52.

35. Gao, C. and Y.G. Chen, *Dishevelled: The hub of Wnt signaling.* Cell Signal, 2010. **22**(5): p. 717-27.

36. Soares, M.L., et al., *Functional studies of signaling pathways in peri-implantation development of the mouse embryo by RNAi.* BMC Dev Biol, 2005. **5**: p. 28.

37. Knowlton, M.N., B.M. Chan, and G.M. Kelly, *The zebrafish band 4.1 member Mir is involved in cell movements associated with gastrulation.* Dev Biol, 2003. **264**(2): p. 407-29.

38. LaMonica, K., M. Bass, and L. Grabel, *The planar cell polarity pathway directs parietal endoderm migration.* Dev Biol, 2009. **330**(1): p. 44-53.

39. Ma, L. and H.Y. Wang, *Mitogen-activated protein kinase p38 regulates the Wnt/cyclic GMP/Ca2+ non-canonical pathway.* J Biol Chem, 2007. **282**(39): p. 28980-90.

40. Kohn, A.D. and R.T. Moon, *Wnt and calcium signaling: beta-catenin-independent pathways.* Cell Calcium, 2005. **38**(3-4): p. 439-46.

41. Liu, T., et al., *Activation of the beta-catenin/Lef-Tcf pathway is obligate for formation of primitive endoderm by mouse F9 totipotent teratocarcinoma cells in response to retinoic acid.* J Biol Chem, 2002. **277**(34): p. 30887-91.

42. Drdova, B. and J. Vachtenheim, *A role for p21 (WAF1) in the cAMP-dependent differentiation of F9 teratocarcinoma cells into parietal endoderm.* Exp Cell Res, 2005. **304**(1): p. 293-304.

43. Yanes, O., et al., *Metabolic oxidation regulates embryonic stem cell differentiation.* Nat Chem Biol, 2010. **6**(6): p. 411-7.

44. Hecker, L., et al., *NADPH oxidase-4 mediates myofibroblast activation and fibrogenic responses to lung injury.* Nat Med, 2009. **15**(9): p. 1077-81.

45. Xiao, Q., et al., *Embryonic stem cell differentiation into smooth muscle cells is mediated by Nox4-produced H2O2.* Am J Physiol Cell Physiol, 2009. **296**(4): p. C711-23.

46. Adachi, Y., et al., *Oncogenic Ras upregulates NADPH oxidase 1 gene expression through MEK-ERK-dependent phosphorylation of GATA-6.* Oncogene, 2008. **27**(36): p. 4921-32.

47. Kajla, S., et al., *A crucial role for Nox 1 in redox-dependent regulation of Wnt-beta-catenin signaling.* FASEB J, 2012. **26**(5): p. 2049-59.

Curriculum Vitae

Leanne Sandieson

Education

Master of Science
University of Western Ontario, London, ON **2010-2012**
- Developmental Biology

Bachelor of Science
University of Waterloo, Waterloo, ON **2006-2010**
- Honours Biology

Research Experience

Graduate Student **2010-2012**
University of Western Ontario
- Thesis Title: Nucleoredoxin and Wnt signaling in F9 cells

Work and Volunteer Experience

Undergraduate Teaching Assistant **2010-2012**
University of Western Ontario
Courses:
- Introductory Biology Lab and Tutorial
- Organismal Physiology Lab and Tutorial
- Genetics Tutorial

Research Assistant for **2009-2010**
Professor Mendis-Millard
University of Waterloo
Assisting with transcribing interviews for
comparing biosphere reserves

Physiotherapist Assistant (Volunteer)
AIM Health Group (Waterloo) **2008**

Awards

- University of Western Ontario Graduate Research Scholarship
- University of Western Ontario Faculty Dependant Scholarship
- University of Waterloo Entrance Scholarship